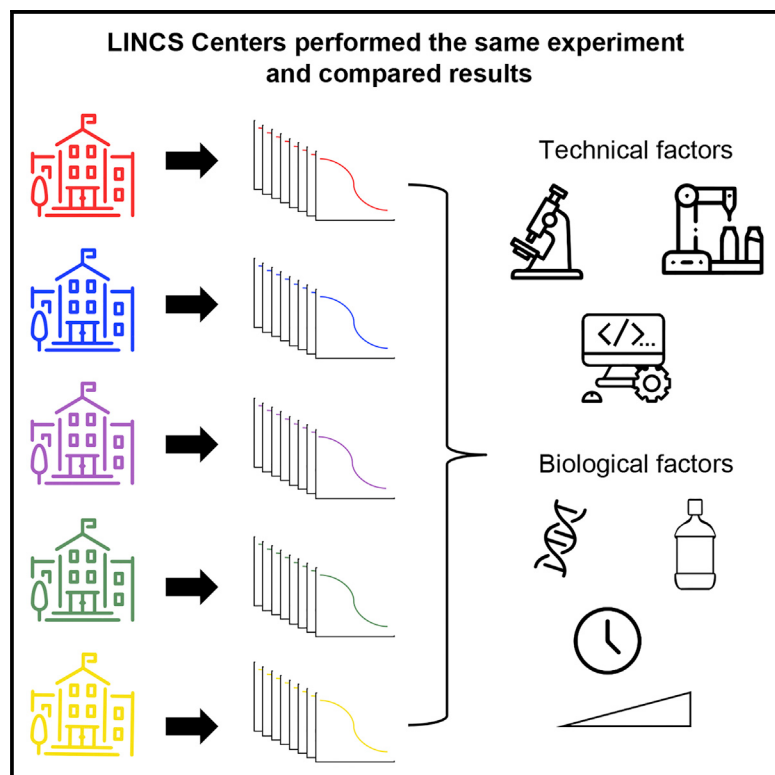


Cell Systems

A Multi-center Study on the Reproducibility of Drug-Response Assays in Mammalian Cell Lines

Graphical Abstract



Authors

Mario Niepel, Marc Hafner,
Caitlin E. Mills, ..., Marc R. Birtwistle,
Laura M. Heiser, Peter K. Sorger

Correspondence

mbirtwi@clemson.edu (M.R.B.),
heiserl@ohsu.edu (L.M.H.),
peter_sorger@hms.harvard.edu (P.K.S.)

In Brief

Factors that impact the reproducibility of experimental data are poorly understood. Five NIH-LINCS centers performed the same set of drug-response measurements and compared results. Technical and biological variables that impact precision and reproducibility and are also sensitive to biological context were the most problematic.

Highlights

- Implementing FAIR data standards requires identification of experimental confounders
- Five labs performed the same experiment on mammalian cells and compared results
- Several factors affecting reproducibility were explored
- Biological context had an unexpected impact on the robustness of cell-based assays



A Multi-center Study on the Reproducibility of Drug-Response Assays in Mammalian Cell Lines

Mario Niepel,^{1,4,8} Marc Hafner,^{1,5,8} Caitlin E. Mills,^{1,8} Kartik Subramanian,^{1,8} Elizabeth H. Williams,^{1,7} Mirra Chung,¹ Benjamin Gaudio,¹ Anne Marie Barrette,² Alan D. Stern,² Bin Hu,² James E. Korkola,³ LINCS Consortium, Joe W. Gray,³ Marc R. Birtwistle,^{2,6,*} Laura M. Heiser,^{3,9,*} and Peter K. Sorger^{1,*}

¹Laboratory of Systems Pharmacology, HMS LINCS Center, Harvard Medical School, Boston, MA 02115, USA

²Department of Pharmacological Sciences, Drug Toxicity Signature Generation (DToxS) LINCS Center, Icahn School of Medicine at Mount Sinai, One Gustave L. Levy Place, Box 1603, New York, NY 10029, USA

³Microenvironment Perturbagen (MEP) LINCS Center, OHSU Center for Spatial Systems Biomedicine, Oregon Health & Sciences University, Portland, OR 97201, USA

⁴Present address: Ribon Therapeutics, Inc, 99 Hayden Avenue, Lexington, MA 02421, USA

⁵Present address: Department of Bioinformatics & Computational Biology, Genentech, Inc, South San Francisco, CA 94080, USA

⁶Present address: Department of Chemical and Biomolecular Engineering, Clemson University, 206 S. Palmetto Blvd., Clemson, SC 29634, USA

⁷Present address: Department of Data Sciences, Dana-Farber Cancer Institute, Boston, MA 02115, USA

⁸These authors contributed equally

⁹Lead Contact

*Correspondence: mbirtwi@clemson.edu (M.R.B.), heiserl@ohsu.edu (L.M.H.), peter_sorger@hms.harvard.edu (P.K.S.)

<https://doi.org/10.1016/j.cels.2019.06.005>

SUMMARY

Evidence that some high-impact biomedical results cannot be repeated has stimulated interest in practices that generate findable, accessible, interoperable, and reusable (FAIR) data. Multiple papers have identified specific examples of irreproducibility, but practical ways to make data more reproducible have not been widely studied. Here, five research centers in the NIH LINCS Program Consortium investigate the reproducibility of a prototypical perturbational assay: quantifying the responsiveness of cultured cells to anti-cancer drugs. Such assays are important for drug development, studying cellular networks, and patient stratification. While many experimental and computational factors impact intra- and inter-center reproducibility, the factors most difficult to identify and control are those with a strong dependency on biological context. These factors often vary in magnitude with the drug being analyzed and with growth conditions. We provide ways to identify such context-sensitive factors, thereby improving both the theory and practice of reproducible cell-based assays.

INTRODUCTION

Making biomedical data more findable, accessible, interoperable, and reusable (the FAIR principles) (Wilkinson et al., 2016) promises to improve how laboratory experiments are performed and interpreted. Adoption of FAIR approaches also responds to concerns from industrial and academic groups about the reproducibility and utility of biomedical research (Arrowsmith, 2011;

Baker, 2016; Begley and Ellis, 2012; Prinz et al., 2011) and the adequacy of data-reporting standards (Errington et al., 2014; Morrison, 2014). Several efforts have been launched to repeat published work (<https://f1000research.com/channels/PRR>), most prominently the Science Exchange Reproducibility Initiative (<http://validation.scienceexchange.com/#/reproducibility-initiative>). The results of such reproducibility experiments have themselves been controversial (eLife Editorial, 2017; Ioannidis, 2017; Nature Editorial, 2017; Nosek and Errington, 2017).

Rather than focus on a specific published result, the current paper investigates the reproducibility of a prototypical class of cell-based experiments. The research was made possible by the NIH Library of Network-Based Cellular Signatures Program (LINCS) (<http://www.lincsproject.org/>) and is consistent with its overall goals: generating datasets that describe the responses of cells to perturbation by small-molecule drugs, components of the microenvironment, and gene depletion or overexpression. For such datasets to be broadly useful, they must be reproducible. The experiment analyzed in this paper involves determining how tissue culture cells respond to small-molecule anti-cancer drugs across a dose range. Such experiments compare pre- and post-treatment cell states and require selection of cell types, assay formats, and time frames; they are therefore prototypical of perturbational biological experiments in general. Drug-response assays are widely used in preclinical pharmacology (Cravatt and Gottesfeld, 2010; Schenone et al., 2013) and in the study of cellular pathways (Barretina et al., 2012; Garnett et al., 2012; Heiser et al., 2012).

Cultured cells are typically exposed to anti-cancer drugs or drug-like compounds for several days (commonly three) and the number of viable cells is then determined, either by direct counting using a microscope or by performing a surrogate assay such as CellTiter-Glo (Promega), which measures ATP levels in a cell lysate. With some important caveats, viable cell number is proportional to the amount of ATP in a lysate prepared from those cells (Tolliday, 2010). Several large-scale datasets



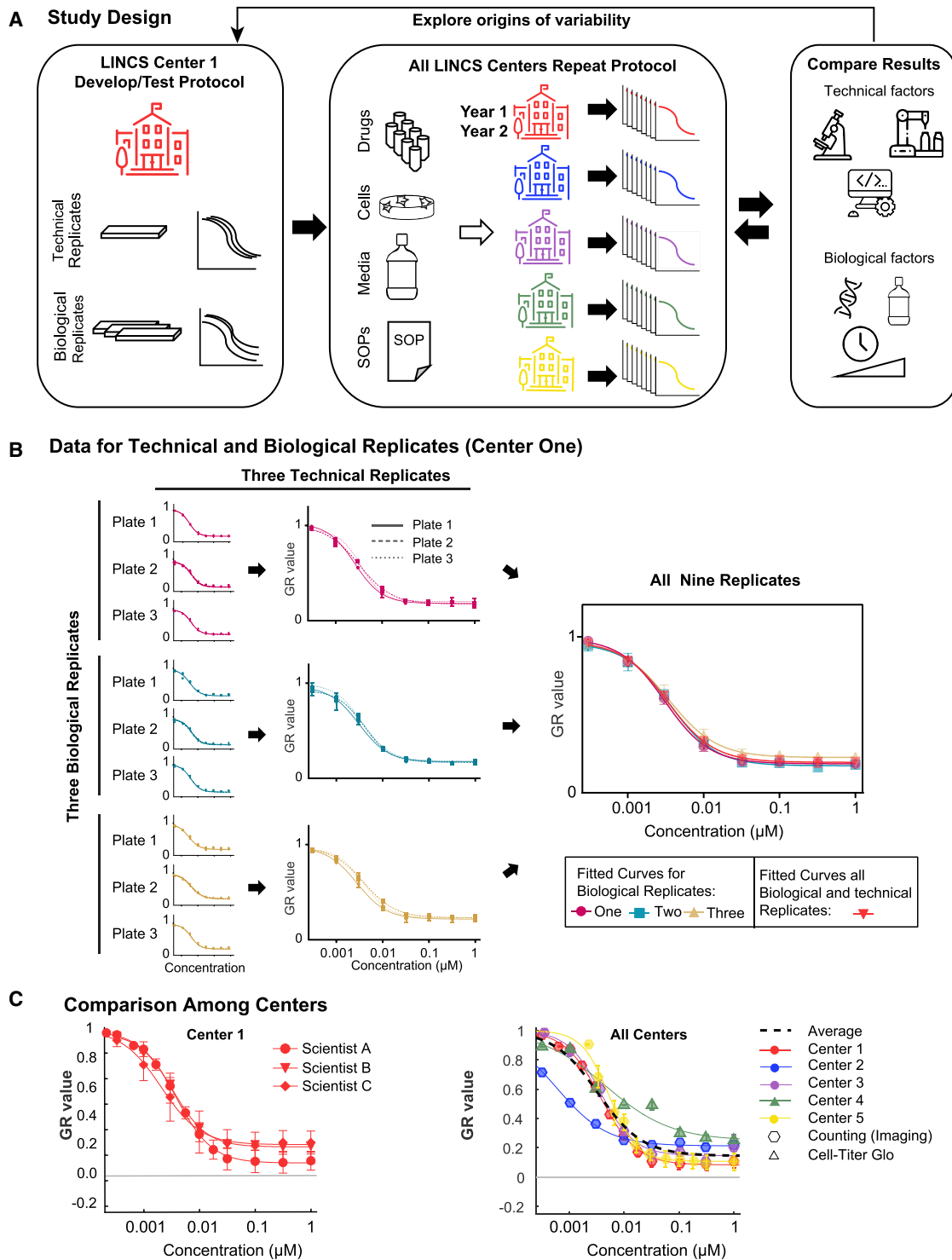


Figure 1. Overview of Workflow

(A) Center one defined the experimental protocol and established within-center reproducibility by assessment of technical (different wells, plates, same day) and biological (different days) replicates. Common stocks of drugs, cells, and media, as well as a standard experimental protocol, were distributed to each of the five data-generation centers. Center one explored the various technical and biological drivers of variability. This information was fed back to the other centers to refine their dose-response measurements.

(B) Dose-response curves of MCF10A treated with the MEK1/2 inhibitor Trametinib from a typical experiment showing technical and biological replicates. Technical replicates at the well (triplicate wells per plate) and plate (triplicate plates per experiment) levels make up biological replicates (repeats collected on different days in the same laboratory). The red triangles represent the average of the three biological replicates shown. Error bars represent SD of the mean.

(legend continued on next page)

describing the responses of hundreds of cell lines to libraries of anti-cancer drugs have recently been published (Barretina et al., 2012; Garnett et al., 2012; Haverty et al., 2016; Seashore-Ludlow et al., 2015), but their reproducibility and utility have been debated (Bouhaddou et al. 2016; CCLE Consortium et al., 2015; Haibe-Kains et al. 2013).

Five experimentally focused LINCS Data and Signature Generation centers (DSGCs) measured the sensitivity of the widely used, non-transformed MCF 10A mammary epithelial cell line to eight small-molecule drugs having different protein targets and mechanisms of action. One DSGC (hereafter “center one”) was charged with studying possible sources of irreproducibility identified by inter-center comparison. Investigators in center one had previously shown that conventional drug response measures such as IC_{50} are confounded by variability in rates of cell proliferation arising from variation in plating density, fluctuation in media composition, and intrinsic differences in cell division times (Hafner et al., 2016, 2017a). We corrected for these and other known confounders using the growth rate inhibition (GR) method (Hafner et al., 2016, 2017b; Niepel et al., 2017), thereby focusing the current study on sources of irreproducibility that remain poorly understood. Individual centers were provided with identical aliquots of MCF 10A cells, drugs, and media supplements, as well as a detailed experimental protocol and data analysis procedures (Figure 1A), *Supplemental Experimental Procedures*. Some variation in the implementation of the protocol was inevitable because not all laboratories had access to the same instruments or the same level of technical expertise; in our view, this is a positive feature of the study because it more fully replicates “real-world” conditions.

In initial experiments, we observed center-to-center variation in GR_{50} measurements of up to 200-fold. Systematic studies revealed factors most likely to be responsible for this variation. In contrast to several recent studies emphasizing genetic instability as a source of variability in sensitivity to anti-cancer drugs (Ben-David et al., 2018), genetic drift did not play a significant role in our studies. Instead, irreproducibility arose from a subtle interplay between experimental methods and poorly characterized sources of biological variation and, to a lesser extent, differences in data analysis (image processing) algorithms. Based on these findings, newly trained technical staff without previous exposure to our protocol could obtain results indistinguishable from assays performed 2 years previously by others. Thus, a sustained commitment to characterizing and controlling for variability in perturbation experiments is both necessary and sufficient to obtain reproducible data.

RESULTS

Measuring Drug Responses in Collaboration

To establish the single-center precision of dose-response assays, center one performed technical and biological replicate measurements using MCF 10A cells and the MEK1/2 kinase inhibitor Trametinib at eight concentrations between 0.33 nM and 1 μ M (Fig-

ures 1B and 1C). For technical replicates, multiple drug dilution series were assayed on one or more microtiter plates on the same day. For biological replicates, three sets of assays were performed, separated by a minimum of one cell passage; each biological replicate involved three technical replicates. In all cases, viable cell number was determined by differentially staining live and dead cells, collecting fluorescence images from each well, segmenting images using software, and then counting all viable cells in all wells (Hafner et al., 2016; Niepel et al., 2017). Sigmoidal curves were fitted to the data and four response metrics derived: potency (GR_{50}), maximal efficacy (GR_{max}), slope of the dose response curve (Hill Coefficient or h_{GR}), and the integrated area over this curve (GR_{AOO}). Fitting procedures and response metrics have been described in detail previously (Hafner et al., 2016, 2017b) (Figure S1A), and all routines and data can be accessed on-line or via download at <http://www.grcalculator.org/>.

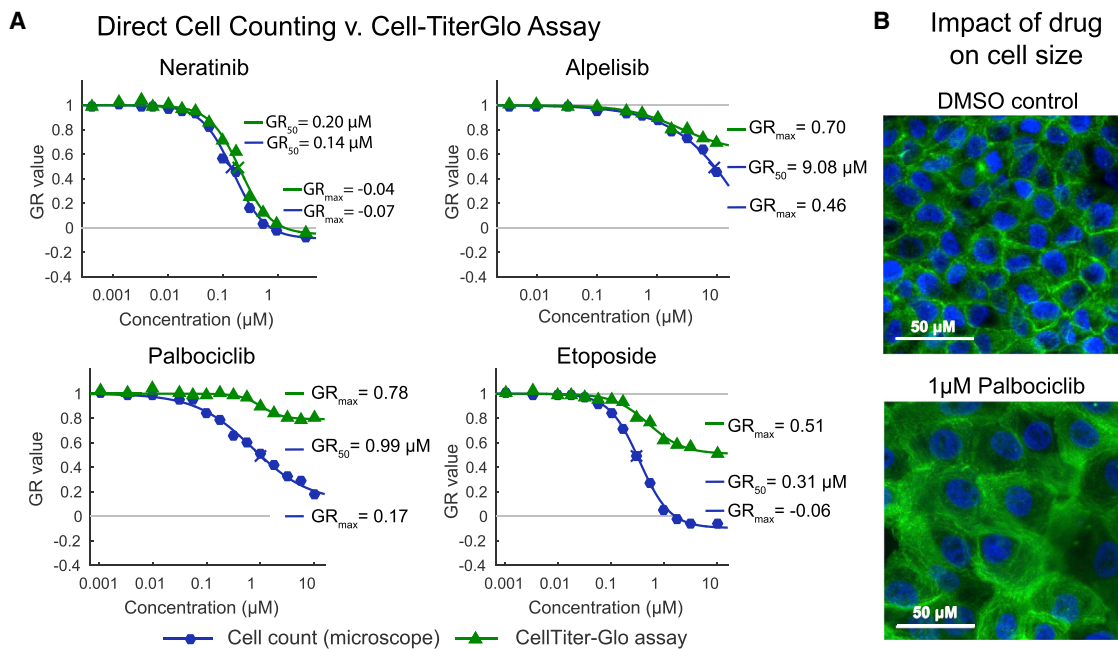
We found that response curves for technical replicates were very similar (Figure 1B), showing that purely procedural error resulting from inaccurate pipetting, non-uniform plating, errors in cell counting, etc., were small. Variability in biological replicates as measured by drug potency ($\log_{10}(GR_{50})$ values) and efficacy (GR_{max} values) was within 1.4 standard deviations for center one (Figure S2) across three different laboratory scientists.

To measure reproducibility across laboratories, while controlling for variation in reagent and genotype, a single center distributed to all other centers identical MCF 10A aliquots, drug stocks, and media additives, as well as a detailed experimental protocol optimized for the cell line-drug pairs under study. This protocol included optimal plating densities, dose-ranges and separation between doses for reliable curve fitting. When individual centers first performed these assays, up to 200-fold variability in GR_{50} values was observed (Figure S3). Differences of this magnitude have previously been observed for large-scale dose-response studies performed by different research teams (Haibe-Kains et al., 2013). To understand the origins of the observed irreproducibility we performed directed and controlled experiments in center one.

Technical Drivers of Variability

First, we studied the origins of the large inter-center variability in estimation of GR_{max} for the topoisomerase inhibitor Etoposide and CDK4/6 inhibitor Palbociclib. We ascertained that one center had used the CellTiter-Glo ATP-based assay and a luminescence plate reader as a proxy for counting the number of viable cells in a microscope. CellTiter-Glo is among the most commonly used assays for measuring cell viability and was therefore a logical substitute for direct cell counting. However, when we performed side-by-side experiments we found that dose-response curves and GR metrics computed from image-based direct cell counts and CellTiter-Glo were not the same: GR_{max} values (which are unit-less and range from -1 to 1) for the topoisomerase inhibitor Etoposide and CDK4/6 inhibitor Palbociclib differed by 0.61 and 0.57, respectively, for the two assays (GR_{50} values could not be determined for CellTiter-Glo data because $GR > 0.5$ under all conditions tested (Figure 2A).

(C) Independent experiments performed in center one, and in all centers (averages of two or more biological replicates). Circles represent the original dataset, triangles represent data collected by a new technician 2 years after the initial data collection [data shown in (B)], and diamonds represent independently collected data in center one. Inter-center replicates (averages of one or more biological replicates) performed independently at each center. Error bars represent the standard deviation of the mean. See also Figure S1.



C Irregularity in cell count across a microtiter plate

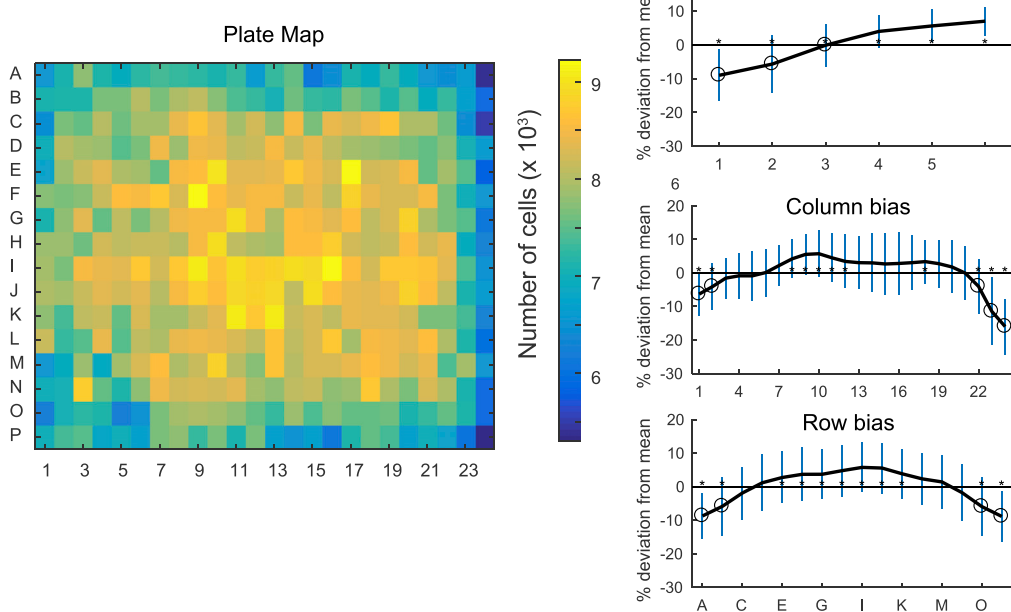
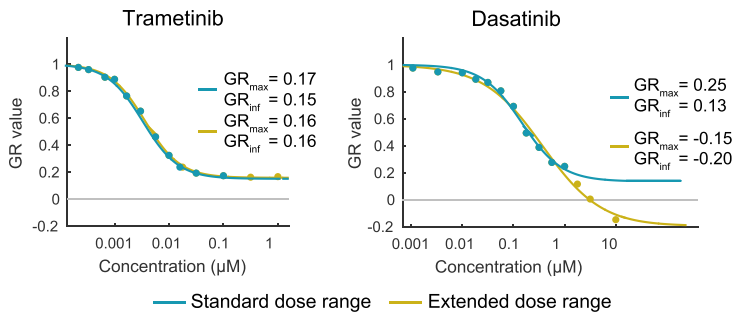
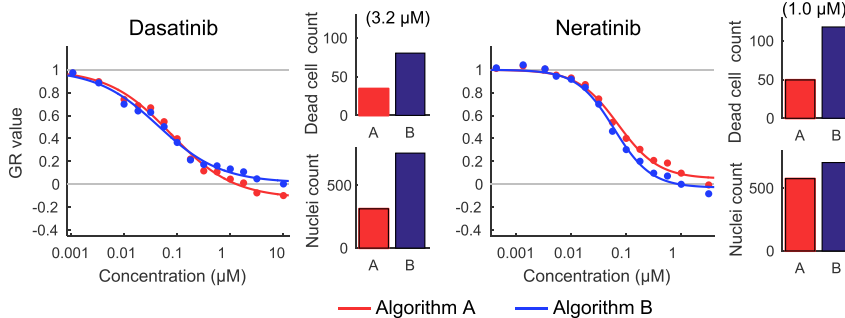


Figure 2. Experimental Causes of Variability

(A) Dose-response curves of MCF 10A cells treated with four different drugs measured by image-based cell count or ATP content (CellTiter-Glo) on the same day by center one, which is equivalent to technical replicates. Note the GR_{50} value for alpelisib as measured by CellTiterGlo was not defined.

(B) Representative images of MCF 10A cells treated with vehicle control (DMSO) or 1 μM Palbociclib. Cells were stained with Hoechst and phalloidin. Images have been contrast adjusted.

(C) Uneven growth of MCF 10A cells in a 384-well plate over the course of 3 days that demonstrates the presence of edge effects. In the heatmap, color represents the number of cells per well, as assessed by imaging. Plots show deviation from mean number (for the full plate based on the distance from the edge, by column, or by row). Error bars represent the standard deviation. Asterisks indicate the row or column differs significantly from all others. See also Figure S2.

A Impact of dose range on response parameters**B Impact of image processing algorithm on cell count**

In contrast, in the case of the EGFR inhibitor Neratinib and the PI3K inhibitor Alpelisib, the differences were smaller, varying by 0.03 and 0.24, respectively. This finding likely explains some of the inter-center differences observed in drug response metrics (Figure S3).

It is known that CellTiter-Glo and direct cell counts are poorly correlated when drugs cause large changes in cell size or alter ATP metabolism, thereby changing the relationship between ATP level in a cell extract and viable cell number (Figure 2B for Palbociclib) (Harris et al., 2016a; Salani et al., 2013; Soliman et al., 2016). The magnitude of this effect depends on the drug being assayed and also on the cell line (Niepel et al., 2017); as a consequence, direct cell counting and CellTiter-Glo can be substituted for each other in some cases but not in others. Thus, a change in protocol justified by pilot studies on a limited number of cell lines and drugs can be problematic when the number or chemical diversity of drugs is increased. In this context, we note that counting viable cells by microscopy is both more direct and cheaper as a measure of viability than ATP levels; CellTiter-Glo is used in place of counting primarily because it is perceived as being easier to perform. The problem is not with CellTiter-Glo itself, which can be reproducible when correctly calibrated, but with equating reduced ATP levels with reduced cell number. Situations in which ATP levels fall in viable or dividing cells might be of interest biologically but identifying these situations requires performing CellTiter-Glo and cell counting assays in parallel.

Edge effects and non-uniform cell growth are a second substantial source of variation in cell based studies performed in microtiter plates (Bushway et al., 2010; Coyle et al., 1989) arising from temperature gradients and uneven evaporation of media. We have observed a variety of irregularities in plating and cell

Figure 3. Technical Causes of Variability

- (A) Dose-response curves of MCF 10A cells treated with Trametinib or Dasatinib fitted to either the extended dose range (up to 1 μM and 10 μM , respectively) or omitting the last order of magnitude.
- (B) Results of cell counting for MCF 10A cells treated with Dasatinib or Neratinib using two different image processing algorithms (denoted as A (red) and B (blue)) included in the Columbus image analysis software package.
- (C) Number of dead cells (LIVE/DEAD™ Fixable Red Dead Cell Stain positive) and nuclei (Hoechst positive) counted for MCF 10A cells treated with 3.16 μM Dasatinib or 1 μM Neratinib based on the two different algorithms (corresponding to the plots in C). See also Figures S3 and S4.

growth that often depend on the batch of microtiter plates, even when plates are obtained from a single highly regarded vendor (Niepel et al., 2017). A variety of approaches are available to minimize edge effects (e.g., placing plates in humidified chambers to reduce evaporation from edge wells), but we find that variation in growth is often confined

to specific regions of a plate (Figure 2C) causing systematic errors in dose-response data. Thus, randomized compound dispensing is a valuable way to reduce biases introduced by edge effects and irregular growth. Using an automated liquid-handling robot such as the HP D300e Digital Dispenser, it is possible to dispense compounds directly into microtiter plates in an arbitrary pattern, randomizing the locations of control and technical replicates and converting systematic error into random error, which is more easily modeled (Niepel et al., 2017). The use of washing and dispensing robots also reduces errors that humans make during repetitive pipetting operations; these robots are small, robust, and relatively inexpensive, and their use improves the reproducibility of many medium- and high-throughput cell-based and biochemical studies.

A third variable we explored involves the concentration range over which a drug is assayed and the impact of this range on curve fitting and parameter estimation. For example, when Trametinib, a MEK kinase inhibitor, was assayed over a thousand-fold concentration range, growth of MCF 10A cells was fully arrested at ~30 nM (Figure 3A, left plot): phenotypic response did not change even when the dose was increased 100-fold to 1 μM and thus, increasing the dose range had no effect on curve fitting (Figure 3A, left plot). However, when Dasatinib, a poly-selective SRC-family kinase inhibition, was assayed over a thousand-fold range, curve fitting identified a plateau in GR value between 0.3 to 1 μM , but when the dose range was extended to higher drug concentrations GR values became negative (Figure 3A, right plot). Thus, a dose range that is adequate for analysis of Trametinib is not adequate for Dasatinib. This sort of variation is difficult to identify in a high-throughput experiment and suggests that pilot studies are needed to optimize dose ranges for specific compounds. Such

variation did not impact reproducibility in our inter-center study because all centers used the identical dose series, but dose range did affect the accuracy of GR_{\max} estimation in general.

A fourth source of inter-center variation was apparent among centers that used imaging-based cell counting, particularly when assaying Dasatinib and Neratinib (Figure 3B). Above 1 μM , GR values were reproducibly negative at center one for both drugs but in one other center, GR_{\max} was consistently above 0. Follow-up studies showed that the discrepancy arose from the use of image processing algorithms that included dead cells in the “viable cell count” and from over-counting the number of cells when multi-nucleation occurred (Orth et al., 2011; Röyttä et al., 1987). Differences in drug response GR values could be recapitulated in a single laboratory by using different image processing routines and were also evident by visual inspection of the segmented images (Figure 3B). In retrospect, all centers should have processed images in the same way using Dockerized software (List, 2017), but the necessary routines are often built into manufacturer’s proprietary software, making standardization of image analysis dependent on the availability of primary data. This demonstrates the impact of a relatively subtle interplay between biological and technical sources of variability and the importance of locking down all steps in the data processing pipeline from raw measurements to final parameter estimation.

Biological Factors Impacting Repeatability

Variables that change the biology of drug response, such as media composition, incubation conditions, microenvironment, media volume, and cell density, have been discussed elsewhere (Hafner et al., 2016; Haverty et al., 2016) and were controlled to the greatest extent possible in this study through standardization of reagents and the use of GR metrics. In a truly independent set of assays, experimental variables such as these would need to be considered as additional confounders because it is difficult to fully standardize a reagent as complex as tissue culture media. However, one center performed a preliminary comparison of batches of horse serum, hydrocortisone, cholera toxin, and insulin and found that the effects on drug response were smaller than the sources of variation discussed above.

At the outset of the study, we had anticipated that the origin of the MCF 10A isolate would be an important determinant of drug response. MCF 10A cells have been grown for many years, and karyotyping reveals differences among isolates (Cowell et al., 2005; Kim et al., 2008; Marella et al., 2009; Soule et al., 1990). To investigate the potential impact of genetic drift, we assembled MCF 10A isolates from different laboratories and compared them to each other and to a histone H2B-mCherry-tagged subclone of one of the isolates (Figure S4A); we also examined four subclones from the LINCS MCF 10A master stock. Variation in measured drug response across all isolates and subclones was smaller than what was observed when a single isolate was assayed at different centers. Because highly variable growth rates are a sign of poor technique, we checked doubling times across centers and found them to be similar (Figure S4B). Thus, even though clonal variation can have a substantial effect on drug response and other properties of cultured cells (Ramirez et al., 2016), such variation was not a significant contributor to variability in this study.

To assay the impact of the time of drug exposure on GR values we performed a live-cell experiment in which cell number was measured every 2 h using an automated high-throughput microscope. When we quantified time-dependent GR values over a 12-h moving window we found a substantial effect in some cases but not others. For example, GR values for cells exposed to Etoposide were nearly constant across all doses throughout a 50-h assay period (Figure 4, top left plot), whereas GR values for Neratinib varied from 0 to 1 over the same period (Figures 4, bottom left plot, and S5), with the highest variability at intermediate drug doses. The temporal dependence of drug response is likely to reflect biological adaptation, drug export, and other factors important in drug mechanism of action (Fallahi-Sichani et al., 2017; Fletcher et al., 2010; Hafner et al., 2016; Harris et al., 2016b; Muranen et al., 2012). These factors remain largely unexplored and are likely to contribute to variation in GR values when protocols are not carefully followed.

Final Results

To assess success in identifying and controlling for sources of variability in the measurement of drug-dose response, we performed two sets of tests. First, all measurements were repeated in center one 2 years after the first round of studies by an experienced research scientist (Scientist A from the original study, Figures 1 and S2) and by a newly recruited technical associate (Scientist B) who did not have prior experience with drug-response assays. Data were collected in biological triplicate with each replicate separated by a minimum of one cell passage from the next; each biological replicate was assayed in technical triplicate, as described in Figure 1B. Plates, media, supplements, and serum were all from different batches as compared to the original experiments and cells were recovered from independent frozen stocks. However, the protocol remained the same over the 2-year period and involved the same automated compound dispensing and plate washing procedures.

Data from newly trained Scientist B exhibited similar standard error for biological and technical repeats with a mean standard error for estimation of GR values of 0.012 across all drugs, doses, and repeats. The distribution was long tailed, an apparent consequence of systematic error in assays involving Neratinib (Figure 5A, lower). As shown in Figure 4, GR values for Neratinib are strongly time-dependent and we might therefore expect data for this drug to be sensitive to small variations in procedure. The observed error in GR values corresponds to a difference in the estimation of GR_{50} values of 1.17-fold (mean standard error, which corresponds to a variation of ± 0.07 in $\log_{10}(\text{GR}_{50})$) while the standard error for 90% of GR_{50} values corresponded to a difference of ~ 1.5 -fold (± 0.18 in $\log_{10}(\text{GR}_{50})$) (Figure 5B). For all measurements obtained in center one over a period of 2 years, the mean standard error in GR values was 0.015, which is only slightly higher than the error from Scientist B alone. The standard deviations in $\log_{10}(\text{GR}_{50})$ and GR_{\max} values obtained by Scientist A over a 2-year period were indistinguishable from each other and there was no observable batch effect for any drug (Figure S2). These distributions represent our best estimate of the error associated with measuring drug-dose response using a single protocol and experimental setup but different consumables; this estimate can therefore be incorporated into future

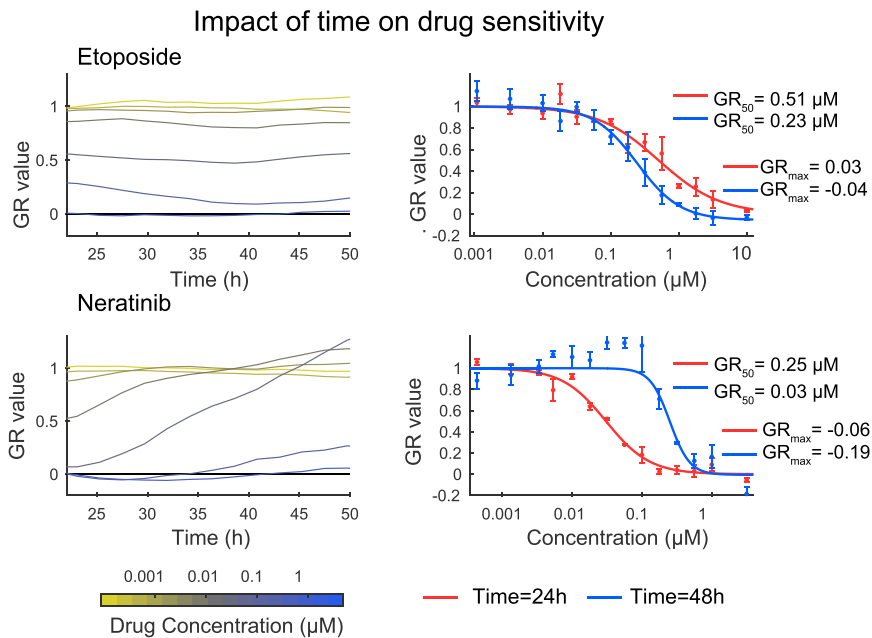


Figure 4. Changes in Drug Response Related to the Underlying Biology

Left: Inhibition of MCF 10A growth (12-h instantaneous GR values) measured in a time-lapse, live-cell experiment involving treatment with multiple doses of Etoposide (top) or Neratinib (bottom). Different colors indicate different drug concentrations ranging from 1 nM (yellow) to 10 μM (blue). Right: Dose-response curves derived from 12-h GR values computed at 24 (red) and 48 h (blue) across three biological repeats. Etoposide displays only modest time-dependent effects (top) while neratinib appears to be more effective at inhibiting growth at early time points as compared to later time points (bottom). Error bars, SD. See also Figure S5.

DISCUSSION

The observation that a large fraction of biomedical research cannot be reproduced is troubling; it handicaps academic and industrial researchers alike and has

error models. In our opinion these values also represent a good level of accuracy and reproducibility.

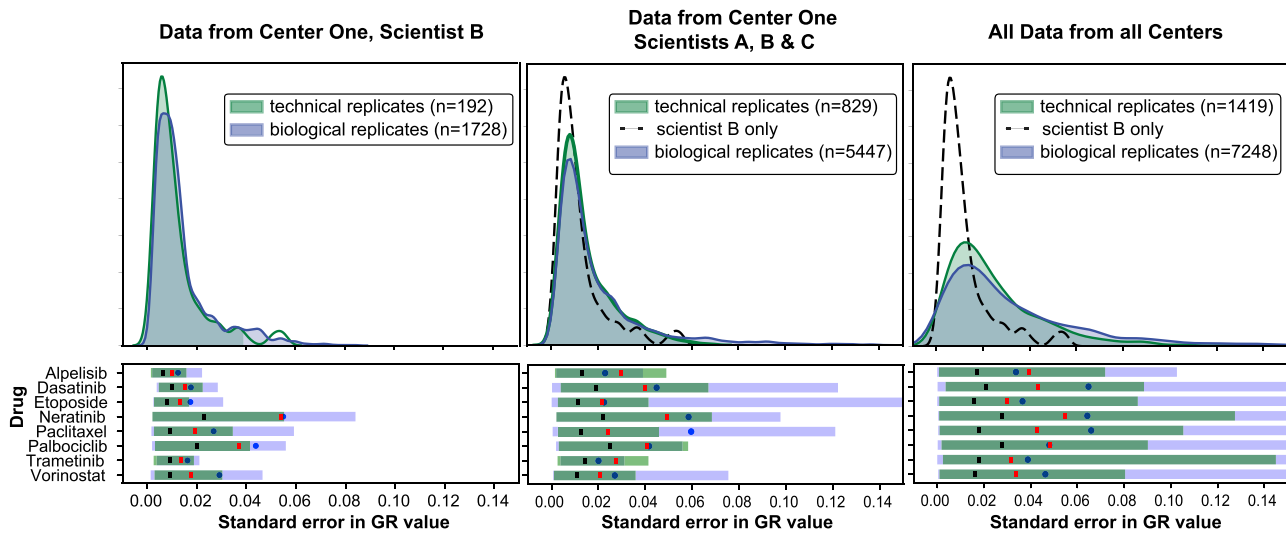
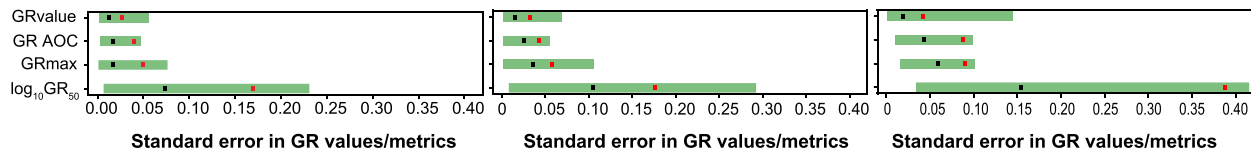
As a second test, centers repeated drug-dose response measurements using their closest approximation to the standard protocol. One center used CellTiter-Glo rather than direct cell counting to estimate viable cell number. Use of this method resulted in greater deviation from the results in center one, as expected from the studies shown in Figures 2, 3, 4, 5, and 6 (e.g., technical error in the CellTiter-Glo data from center four exceeded that of all other centers). Despite such differences in procedure inter-center variability at the end of the study was lower than at the outset, with a standard error in GR value measurement ~2-fold higher than in center one and errors in the estimation of GR₅₀ of ~2 standard deviations. The mean standard error for log₁₀(GR₅₀) across all drugs was ± 0.15 while the standard error for 90% of measured GR₅₀ values was within ~2.5-fold (± 0.38 in log₁₀(GR₅₀)) (Figure 5B).

The distribution of standard errors in GR values is long tailed. Although the mean standard errors for technical and biological replicates are comparable, error associated with biological replicates has a longer tail, as illustrated by the cases where the upper 10th to 5th percentile error across biological replicates was greater than the error in technical replicates (Figure 5A, lower panels). For example, center four had consistently high technical variability and low biological variability, possibly a result of their use of the CTG assay. Overall, the largest identifiable source of error in the final data arose from use of the CTG assay as opposed to direct cell counting (Figure 6).

From these data we conclude that it is possible for previously inexperienced individuals to measure drug-dose response with high reliability over an extended period of time and that multiple centers can approximate this level of reproducibility. However, deviations from an SOP (see *Supplemental Experimental Procedures*) with respect to automation and type of assay, which might be necessary for practical reasons, can have a substantial negative impact.

generated extensive comment in the scientific and popular press (Arrowsmith, 2011; Baker, 2016; Begley and Ellis, 2012; Prinz et al., 2011; Wilkinson et al., 2016). The key question is why such irreproducibility arises and how it can be overcome; in the absence of systematic studies such as ours, FAIR data will remain little more than an aspiration. In this study, we investigated the precision and reproducibility of a prototypical perturbational experiment performed in cell lines: drug dose-response as measured by cell viability. Perturbational experiments are foundational in genetics, chemical biology, and biochemistry, and when they involve human therapeutics, they are also of translational value. A consortium of five geographically dispersed NIH LINCS centers initially encountered high levels of inter-center variability in estimating drug-potency, even when a common set of reagents was used. Subsequent study in a single center uncovered possible sources of measurement error, resulting in a substantial increase in inter-center reproducibility. Nonetheless, the final level of inter-center variability exceeded what could be achieved in a single laboratory over a period of 2 years by three scientists. We ascribe the remaining irreproducibility to differences in compound handling, pipetting, and cell counting that were not harmonized because of the expense of acquiring the necessary instrumentation and a belief—belied by the final analysis—that counting cells is such a simple procedure that different assays can be substituted for each other without consequence. We believe the final level of intra- and inter-center precision we achieved exceeds the norm for this class of experiments in the current literature (although this is not easy to prove) and that our findings therefore provide a roadmap for future studies of reproducibility in other settings.

At the outset of the study we had hoped that comparison of data across centers would serve to identify the specific biological, experimental, and computational factors that had the largest impact on data reproducibility. However, we discovered that most examples of irreproducibility are themselves irreproducible and that technical factors responsible for any specific outlier

A Error distributions for individual GR Values**B Error in computed GR metrics****Figure 5. Technical and Biological Variability in Estimating GR Values and Metrics**

(A) The kernel density estimate (KDE) of the standard error (SE) for measurement of GR values across technical (green curve) or biological (blue curve) replicates for all drugs and doses. The left panel depicts data from center one, scientist B (performed in 2018); the middle panel shows four sets of measurements from all scientists in center one (performed between 2016–2018); and the right panel all data from all centers. The distribution of technical error for Scientist B is duplicated in the middle and right panels as a black dotted line to facilitate comparison. Data for these distributions were derived from GR values for each dose and replicate, not GR metrics obtained from curve fitting. The number of GR value data points used to compute SE is detailed in [STAR Methods](#). The number of SE data points that constitute each KDE is shown in the legend; for the left panel this is 192 SE data points (8 doses × 8 drugs × 3 biological repeats). The lower section of each panel depicts the error in GR value measurements across technical replicates (green) and biological replicates (blue) for each individual drug.

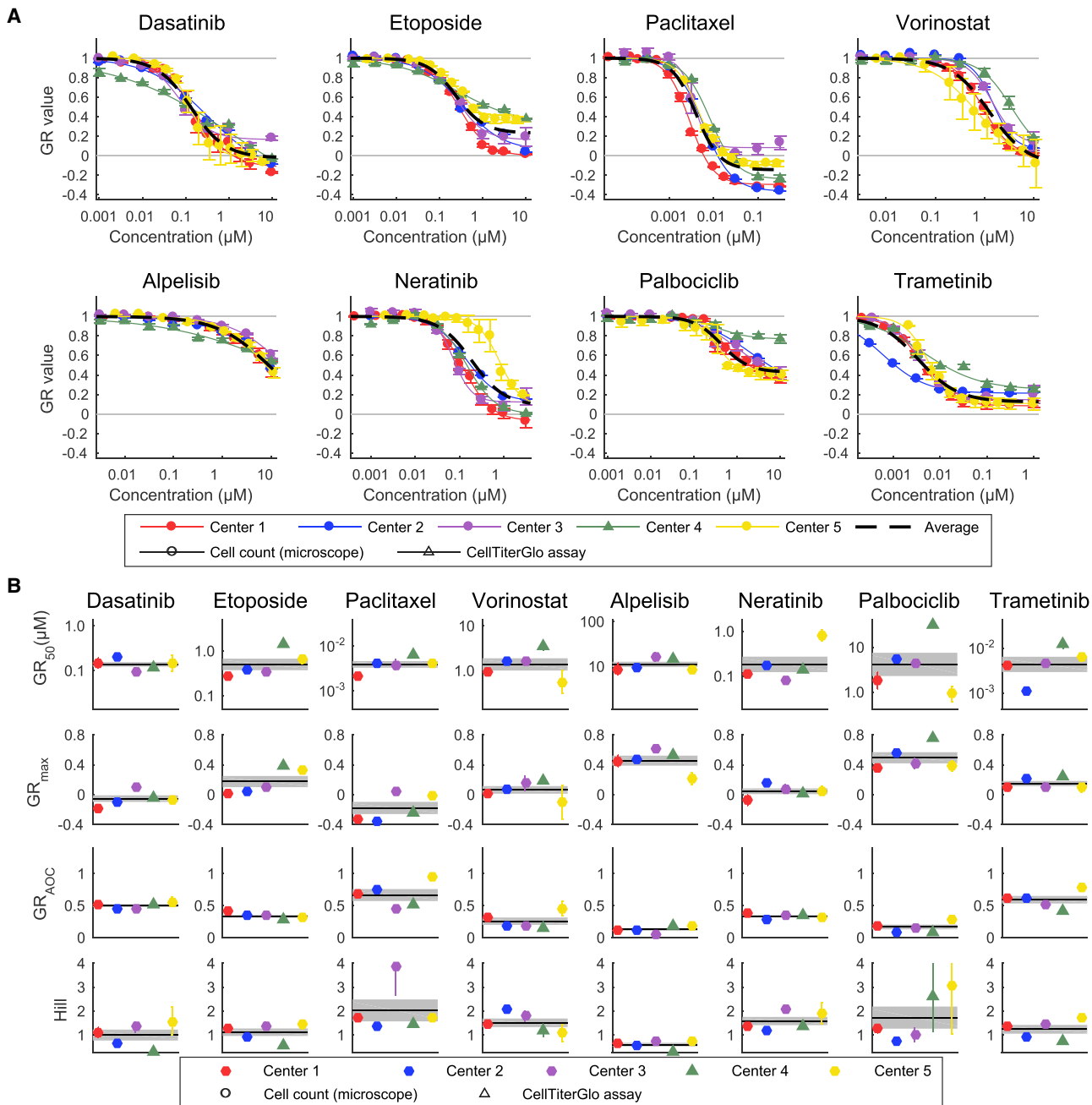
(B) The range of SE in GR values compared to the SE in corresponding GR metrics (GR_{max}, area over the GR curve (GR AOC), and log₁₀GR₅₀) for all drugs. The black vertical line (A, lower plots, and B) is the mean technical error for a given drug and the red vertical line demarcates the 90th percentile error across technical replicates (meaning that the error for 90% of GR values or GR metrics is below that value); a blue circle demarcates 90th percentile error across biological replicates.

measurement are difficult to pin down. We therefore undertook a systematic study of the assay itself, in a single center, with an eye to identifying those variables with the greatest impact on reproducibility. We found that these variables differed from what we expected a priori. For example, isolate-to-isolate differences in MCF 10A cultures had less of an effect on drug response assays ([Figure S4A](#)) than the ways in which drugs and cells were plated into multi-well plates and counted ([Figures 2 and 3](#)).

In general, we found that irreproducibility most commonly arose from unexpected interplay between experimental protocol and true biological variability. For example, estimating cell number from ATP levels using the CellTiter-Glo assay produces very similar results to direct cell counting with a microscope in the case of Neratinib, but this is not true for Etoposide or Palbociclib ([Figure 2A](#)). The discrepancy most likely arises because ATP levels in lysates of drug-treated cells vary for reasons other than loss of viability; these include changes in cell size and metabolism. We have previously shown that the density at which cells are assayed can have a dramatic effect on drug response ([Haf-](#)

[ner et al., 2016](#)), but this too is context dependent. For some cell line-drug pairs, density has little or no effect, whereas for other pairs it increases drug sensitivity and for yet others it has the opposite effect. This observation has important implications for the design of experiments in which diverse compounds are screened: pilot studies on a limited range of conditions (dose and drug identity in this work) cannot necessarily be extrapolated to large datasets and are not a sound basis for substituting indirect assays for direct assays. The tendency for even experienced investigators to substitute assays for each other, or to implement historical methods rather than standardized protocols (SOPs), is undoubtedly a source of irreproducibility.

Several lines of evidence suggest that context dependence in drug response reflects true changes in the underlying biology and not flaws in assay methodology itself. For example, cell density directly impacts media conditioning and the strength of autocrine signaling, which in turn changes responsiveness to some drugs but not others ([Wilson et al., 2012](#); [Yonesaka et al., 2008](#)). Thus, even in cell lines, drug response is not a

**Figure 6. Variability of the Response Measures across Centers**

(A) Dose-response curves of MCF 10A cells treated with eight drugs measured independently by the five centers (circles represent data from image-based assays and triangles from CellTiter-Glo assays). See Figure S6 for underlying replicates. Dotted black lines show the dose-response curve when all independent replicates were averaged. Error bars represent SD of the mean.

(B) GR metrics describing the sensitivity of MCF 10A cells to eight drugs measured independently by five centers (circles represent data from image-based assays and triangles from CellTiter-Glo assays). The black line shows the mean sensitivity across all centers, and the gray area shows the standard error of the mean computed from the average of each center. For GR₅₀ and GR_{max}, error bars represent the standard deviation of the log₁₀(GR) values. Note that some data are shared between Figures 6 and S3.

simple biological process, and it is easy to envision ways in which changes in measurement procedure that might have no effect in one cell type or biological setting could affect results obtained in other settings. At the current state of knowledge, there is no substitute for empirical studies that carefully assess the

range of conditions over which data remain reliable and precise for cell lines and drugs of interest. Moreover, the most direct assay—not a convenient substitute—should be used to score a phenotype whenever possible. Unfortunately, when the goal is collection of a large dataset, a prerequisite for most

machine-learning approaches, attention to biological factors known to be important from conventional cell biology studies is often de-emphasized in favor of throughput.

Data-processing routines are important for reproducibility (Sandve et al., 2013). Data and data-analysis routines can interact in multiple ways, some of which are clear in retrospect but not necessarily anticipated. For example, collecting eight-point dose-response curves generally represents good practice, but it is essential that the dose range effectively span the GEC₅₀ (the mid-point of the response). When this is not the case (as illustrated by Figure 3A), curve fitting is underdetermined and response metrics become unreliable. In many cases problems with dose range are not evident until an initial assay has been performed and an iterative approach is therefore necessary. Iteration is straightforward in small-scale studies, but more difficult in large-scale screens; for a large dataset, data-processing routines must be developed to automatically identify and flag problems with dose range. Additionally, accurate reporting of dose range is necessary to provide a bound-to-drug sensitivity measurement. Another example of data-processing challenges involves imaging software for automated cell counting: such routines should be optimized for cells that grow and respond to drugs in different ways (Figure 3B) and must be tested for performance at high and low cell densities.

Processing pipelines for the type of data collected in this study are much less developed than the pipelines commonly used for genomics data (Ashley, 2016; Bao et al., 2014; Lam et al., 2011), but much can be learned from the comparison. For example, computational platforms with provenance such as Galaxy (Goecks et al., 2010), or Sage Bionetworks' Synapse (Omberg et al., 2013) have been developed to support data sharing, reproducible analyses, and transparent pipelines, with a primary focus on genomics data. Some of these best practices have already been adapted to the analysis of LINCS dose-response data (see STAR Methods). Image-processing algorithms present a unique challenge in that they are frequently embedded in proprietary software linked to a specific data acquisition microscope, which complicates common analysis across laboratories; publicly available image analysis platforms are preferable (Carpenter et al., 2006).

Elements of a Reproducible Workflow

The elements of a workflow for reproducible collection of dose-response data are fairly simple conceptually (Figure 7A) although not necessarily easy to implement: (1) standardization of reagents, including obtaining cell lines directly from repositories such as the ATCC, performing mass spectrometry-based quality control of small-molecule drugs, and tracking lot numbers for all media additives; (2) standardized data processing starting with raw data and metadata through to reporting of final results; (3) use of automation to improve reliability and enable experimental designs too complex or labor intensive for humans to execute reliably—in many cases, this involves simple and relatively inexpensive bench-top dispensing and washing—and (4) close attention to metrology (analytical chemistry), measurement technology, and internal quality controls. The first two points are obvious, but not all laboratories are equipped in the same way and some data-processing routines are embedded in a non-obvious way in instrument software. In the current work, a major benefit of automation is that it makes random plate layouts

feasible, thereby changing systematic edge effects into random error that has less effect on dose-response curve fitting. In the case of dose-response data, metrology focuses on variability among technical and biological replicates, assessment of edge effects, and outlier detection. Edge effects and other spatial artifacts can be identified by statistical analysis (Mazoure et al., 2017) and plate-wise data visualization (Boutros et al., 2006). Spatial artifacts can then be removed with plate-level normalization such as LOESS/LOWESS smoothing (Boutros et al., 2006; Pelz et al., 2010), spatial autocorrelation (Lachmann et al., 2016), or statistical modeling (Mazoure et al., 2017).

A contribution of the current study is to show that future execution of reproducible drug-dose-response assays in different cell types requires systematic experimentation aimed at establishing the robustness of assays over a full range of biological settings and cell types. Such robustness is distinct from conventional measures of assay performance such as precision or repeatability in a single biological setting (Figure 7B). Testing of this type is not routinely performed for the simple reason that establishing and maintaining robust and reproducible assays is time consuming and expensive: we estimate that reproducibility adds ~20% to the total cost of a large-scale study such as drug-response experiments in panels of cell lines (AlQuraishi and Sorger, 2016). Iterative experimental design is also essential, even though it has been argued that this is not feasible for large-scale studies (Harris, 2017).

Conclusions

A question raised by our analysis is whether, given their variability and context-dependence, drug response assays performed *in vitro* are useful for understanding drug response in other settings, human patients in particular. Concern about the translatability of *in vitro* experiments is long-standing, but we think the current work provides grounds for optimism rather than additional worry. Simply put, if *in vitro* data cannot be reproduced from one laboratory to the next, then it is no wonder that they cannot easily be reproduced in humans; conversely, paying greater attention to accurate and reproducible *in vitro* data are likely to improve translation. Moreover, many of the factors that appear to represent irreproducibility in fact arise from biologically meaningful variation. These include the time-dependence of drug response, the impact of non-genetic heterogeneity at a single-cell level, and the influence of growth conditions and environmental factors. The simple assays of drug response in current use are unable to correct for such variability, and the problem is made worse by “kit-based science” in which technical validation of assays is left to vendors. However, if the challenge of understanding biological variability at a mechanistic level is embraced, it seems likely that we will improve our ability to conduct *in vitro* assays reproducibly and apply data obtained in cell lines to human patients (Goodspeed et al., 2016). We note that RNAi, CRISPR, and other perturbational experiments in which phenotypes are measured in cell culture are likely to involve many of the same variables as the dose-response experiments studied here.

Despite a push for adherence to the FAIR principles there is currently no consensus that the necessary investment is worthwhile, nor do incentives exist in the publication or funding processes for individual research scientists to meet FAIR standards

A Factors affecting precision, reproducibility in this study

Experimental design

- GR Metrics - control for confounding effect of growth on drug response
- Randomize position of drugs on plate - reduce impact of systematic error such as edge effects
- Optimize dose range - ensure accurate curve fitting and GR parameter optimization

Materials and Supplies

- QC drugs - confirm compound identity by LC/MS
- Check multi-well plates - for uniform growth across plates from one batch
- Cell line identity - STR profiling before and after large experiment

Method

- Optimize growth parameters - control for cell density at time of drug addition
- Automate plating- better consistency with liquid handler: Multidrop Combi (Thermo) or similar
- Automate dosing - enables randomization: HP D300 digital drug dispenser (Hewlett Packard)
- Automate washing - more complete washes: EL405x plate washer (BioTek) or similar
- Follow SOP - do not substitute similar assays without careful analysis (e.g CellTiter-Glo for counting)

Data Analysis

- Jupyter notebook - for experimental design and final data
- Dockerized pipelines - for cell segmentation and counting confirm performance against images

● Uniform across all centers
● Non-uniform across centers
● Established significant source of variability
● Established unimportant source of variability in this study
● Good general practice - not specifically tested

B Assay precision, reproducibility and biological robustness

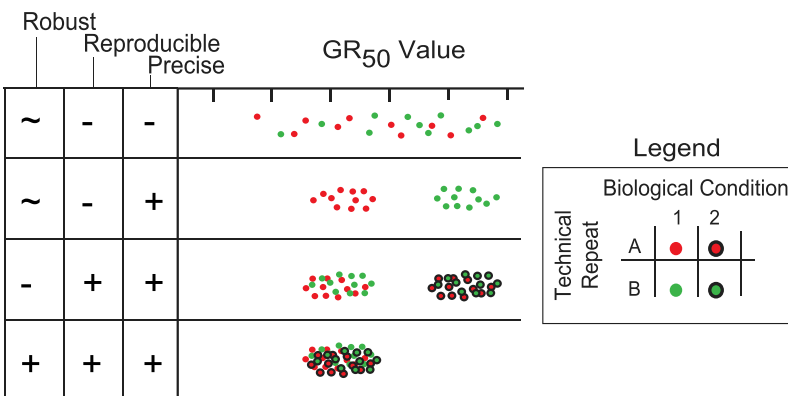


Figure 7. Best Practices for Dose-Response Measurement Experiments

(A) Summary of findings in this and related studies with respect to experimental and technical variability in dose response studies at the experimental design, materials, methods, and analysis stages; “**” indicates sources of variability that have been thoroughly investigated in a previous paper (Hafner et al., 2016).

(B) Differences between precision, robustness, and reproducibility; see text for details.

(AlQuraishi and Sorger, 2016). Data repositories are essential, but we also require better training in metrology, analytical chemistry, and statistical quality control. In developing incentives and training programs, we must also recognize that reproducible research is a public good whose costs are borne by individual investigators and whose benefits are conferred to the community as a whole.

STAR★METHODS

Detailed methods are provided in the online version of this paper and include the following:

- KEY RESOURCES TABLE
- LEAD CONTACT AND MATERIALS AVAILABILITY
 - Materials Availability Statement
- EXPERIMENTAL MODEL AND SUBJECT DETAILS
- METHOD DETAILS
 - Measuring Drug Responses – SOP
- QUANTIFICATION AND STATISTICAL ANALYSIS
- DATA AND CODE AVAILABILITY

SUPPLEMENTAL INFORMATION

Supplemental Information can be found online at <https://doi.org/10.1016/j.cels.2019.06.005>.

LINCS CONSORTIUM

HMS-LINCS: Caroline E. Shamu; **DTox:** Gomathi Jayaraman, Evren U. Azeloglu, Ravi Iyengar, Eric A. Sobie; **MEP-LINCS:** Heidi S. Feiler, Rebecca Smith, Kaylyn Devlin, Gordon B. Mills, Tiera Liby; **LINCS-PCCSE:** Jacob D. Jaffe, Maria Alimova, Desiree Davison, Xiaodong Lu; **LINCS-Transcriptomics:** Todd R. Golub, Aravind Subramanian; **NeuroLINCS:** Brandon Shelley, Clive N. Svendsen; **DCIC:** Avi Ma'ayan, Mario Medvedovic. For a complete list of consortium affiliations, please see Document S2.

ACKNOWLEDGMENTS

We thank K. Ward for help with automation. This work was funded by grants U54HL127365 to P.K.S.; U54HG008098 to R.I., M.R.B., and E.A.S.; R01-GM104184 to M.R.B.; U54HL127624 to M.M. and A.M.; U54-HG008100 to J.W.G., L.M.H., and J.E.K.; U54-HG008097 to J.D.J.; U54NS091046 to C.N.S.; U54HL127366 to T.R.G. and A.D.S.; and T32GM062754 to A.M.B.

AUTHOR CONTRIBUTIONS

M.N., M.H., C.E.M., K.S., E.H.W., J.E.K., J.W.G., M.R.B., L.M.H., and P.K.S. designed the study and led its execution. M.C., B.G., A.M.B., B.H., and A.D.S. participated in data collection and analysis. All authors edited the manuscript.

DECLARATION OF INTERESTS

Peter K. Sorger is a member of the SAB or Board Of Directors of Merrimack Pharmaceutical, Glencoe Software, Applied Biomath and RareCyt Inc and has equity in these companies. Sorger declares that none of these relationships are directly or indirectly related to the content of this manuscript. Caroline Shamu's spouse is a member of the SAB or Board of Directors of Merrimack Pharmaceutical, Glencoe Software, Applied Biomath and RareCyt Inc and she has equity in these companies. Shamu declares that none of these relationships are directly or indirectly related to the content of this manuscript. Joe W. Gray has licensed technologies to Abbott Diagnostics and Danaher and has ownership positions in PDX Pharmaceuticals and Convergent Genomics. Gray serves as an advisor to New Leaf Ventures and KromaTid. Gray

currently receives research funding or other support from Thermo Fisher (formerly FEI), Zeiss, Danaher (Cepheid), Micron, PDX Pharmaceuticals, Susan G. Komen Foundation, the Prospect Creek Foundation, the NCI Cancer Systems Biology Program, the NCI Human Tumor Atlas Program and the NIH LINCS program. Mario Niepel is an employee of Ribon Therapeutics. Niepel declares that this relationship is not directly or indirectly related to the content of this manuscript. Marc Hafner is an employee of Genentech, Inc. Hafner declares that this relationship is not directly or indirectly related to the content of this manuscript. Gordon Mills is a consultant for or SAB member of AstraZeneca, Chrysalis, ImmunoMET, Ionis, Mills Institute for Personalized Care (MIPCC), Nuevolution, PDX Pharma, SignalChem Lifesciences, Sympogen, and Tarveda. Gordon Mills has financial relationships with Catena Pharmaceuticals, ImmunoMet, SignalChem, Spindletop Ventures, and Tarveda. Gordon Mills has licensed technology to Myriad Genetics and Nanostring. Gordon Mills currently receives research funding from AztraZeneca, Karus Therapeutics, Nanostring, Pfizer, Tesaro, as well as the following foundations: Adelson Medical Research Foundation, Breast Cancer Research Foundation, Komen Research Foundation, Ovarian Cancer Research Foundation, Prospect Creek Foundation. Todd Golub is a paid consultant to Foundation Medicine, Sherlock Biosciences, and GlaxoSmithKline.

Received: January 22, 2018

Revised: February 1, 2019

Accepted: June 12, 2019

Published: July 10, 2019

REFERENCES

- AlQuraishi, M., and Sorger, P.K. (2016). Reproducibility will only come with data liberation. *Sci. Transl. Med.* 8, 339ed7, Seventh Edition.
- Arrowsmith, J. (2011). Trial watch: Phase II failures: 2008–2010. *Nat. Rev. Drug Discov.* 10, 328–329.
- Ashley, E.A. (2016). Towards precision medicine. *Nat. Rev. Genet.* 17, 507–522.
- Baker, M. (2016). Biotech giant publishes failures to confirm high-profile science. *Nature* 530, 141.
- Bao, R., Huang, L., Andrade, J., Tan, W., Kibbe, W.A., Jiang, H., and Feng, G. (2014). Review of current methods, applications, and data management for the bioinformatics analysis of whole exome sequencing. *Cancer Inform.* 13, 67–82.
- Barretina, J., Caponigro, G., Stransky, N., Venkatesan, K., Margolin, A.A., Kim, S., Wilson, C.J., Lehár, J., Kryukov, G.V., Sonkin, D., et al. (2012). The Cancer Cell Line Encyclopedia enables predictive modelling of anticancer drug sensitivity. *Nature* 483, 603–607.
- Begley, C.G., and Ellis, L.M. (2012). Drug development: raise standards for preclinical cancer research. *Nature* 483, 531–533.
- Ben-David, U., Siranosian, B., Ha, G., Tang, H., Oren, Y., Hinohara, K., Strathdee, C.A., Dempster, J., Lyons, N.J., Burns, R., et al. (2018). Genetic and transcriptional evolution alters cancer cell line drug response. *Nature* 560, 325–330.
- Bouhaddou, M., DiStefano, M.S., Riesel, E.A., Carrasco, E., Holzapfel, H.Y., Jones, D.C., Smith, G.R., Stern, A.D., Somani, S.S., Thompson, T.V., et al. (2016). Drug response consistency in CCLE and CGP. *Nature* 540, E9–E10.
- Boutros, M., Brás, L.P., and Huber, W. (2006). Analysis of cell-based RNAi screens. *Genome Biol.* 7, R66.
- Bushway, P.J., Azimi, B., Heynen-Genel, S., Price, J.H., and Mercola, M. (2010). Hybrid median filter background estimator for correcting distortions in microtiter plate data. *Assay Drug Dev. Technol.* 8, 238–250.
- Carpenter, A.E., Jones, T.R., Lamprecht, M.R., Clarke, C., Kang, I.H., Friman, O., Guertin, D.A., Chang, J.H., Lindquist, R.A., Moffat, J., et al. (2006). CellProfiler: image analysis software for identifying and quantifying cell phenotypes. *Genome Biol.* 7, R100.
- CCLE Consortium, GDSC Consortium and Genomics of Drug Sensitivity in Cancer Consortium (2015). Pharmacogenomic agreement between two cancer cell line data sets. *Nature* 528, 84–87.

- Cowell, J.K., LaDuca, J., Rossi, M.R., Burkhardt, T., Nowak, N.J., and Matsui, S. (2005). Molecular characterization of the t(3;9) associated with immortalization in the MCF10A cell line. *Cancer Genet. Cytogenet.* 163, 23–29.
- Coyle, M.P., Jr., Green, D.P., and Monsanto, E.H. (1989). Advances in carpal bone injury and disease. *Hand Clin.* 5, 471–486.
- Cravatt, B.F., and Gottesfeld, J.M. (2010). Chemical biology meets biological chemistry minireview series. *J. Biol. Chem.* 285, 11031–11032.
- Debnath, J., Muthuswamy, S.K., and Brugge, J.S. (2003). Morphogenesis and oncogenesis of MCF-10A mammary epithelial acini grown in three-dimensional basement membrane cultures. *Methods* 30, 256–268.
- eLife editorial. (2017). The challenges of replication. *eLife* 6, e23693.
- Errington, T.M., Iorns, E., Gunn, W., Tan, F.E., Lomax, J., and Nosek, B.A. (2014). An open investigation of the reproducibility of cancer biology research. *eLife* 3.
- Fallahi-Sichani, M., Becker, V., Izar, B., Baker, G.J., Lin, J.R., Boswell, S.A., Shah, P., Rotem, A., Garraway, L.A., and Sorger, P.K. (2017). Adaptive resistance of melanoma cells to RAF inhibition via reversible induction of a slowly dividing de-differentiated state. *Mol. Syst. Biol.* 13, 905.
- Fletcher, J.I., Haber, M., Henderson, M.J., and Norris, M.D. (2010). ABC transporters in cancer: more than just drug efflux pumps. *Nat. Rev. Cancer* 10, 147–156.
- Garnett, M.J., Edelman, E.J., Heidorn, S.J., Greenman, C.D., Dastur, A., Lau, K.W., Greninger, P., Thompson, I.R., Luo, X., Soares, J., et al. (2012). Systematic identification of genomic markers of drug sensitivity in cancer cells. *Nature* 483, 570–575.
- Goecks, J., Nekrutenko, A., and Taylor, J.; Galaxy Team (2010). Galaxy: a comprehensive approach for supporting accessible, reproducible, and transparent computational research in the life sciences. *Genome Biol.* 11, R86.
- Goodspeed, A., Heiser, L.M., Gray, J.W., and Costello, J.C. (2016). Tumor-derived cell lines as molecular models of cancer pharmacogenomics. *Mol. Cancer Res.* 14, 3–13.
- Hafner, M., Niepel, M., Chung, M., and Sorger, P.K. (2016). Growth rate inhibition metrics correct for confounders in measuring sensitivity to cancer drugs. *Nat. Methods* 13, 521–527.
- Hafner, M., Niepel, M., and Sorger, P.K. (2017a). Alternative drug sensitivity metrics improve preclinical cancer pharmacogenomics. *Nat. Biotechnol.* 35, 500–502.
- Hafner, M., Niepel, M., Subramanian, K., and Sorger, P.K. (2017b). Designing drug-response experiments and quantifying their results. *Curr. Protoc. Chem. Biol.* 9, 96–116.
- Haibe-Kains, B., El-Hachem, N., Birkbak, N.J., Jin, A.C., Beck, A.H., Aerts, H.J., and Quackenbush, J. (2013). Inconsistency in large pharmacogenomic studies. *Nature* 504, 389–393.
- Harris, E.A., Koh, E.J., Moffat, J., and McMillen, D.R. (2016a). Automated inference procedure for the determination of cell growth parameters. *Phys. Rev. E* 93, 012402.
- Harris, L.A., Frick, P.L., Garbett, S.P., Hardeman, K.N., Paudel, B.B., Lopez, C.F., Quaranta, V., and Tyson, D.R. (2016b). An unbiased metric of antiproliferative drug effect in vitro. *Nat. Methods* 13, 497–500.
- Harris, R. (2017). Rigor mortis: how sloppy science creates worthless cures, crushes hope, and wastes billions (Perseus Books Group).
- Haverty, P.M., Lin, E., Tan, J., Yu, Y., Lam, B., Lianoglou, S., Neve, R.M., Martin, S., Settleman, J., Yauch, R.L., et al. (2016). Reproducible pharmacogenomic profiling of cancer cell line panels. *Nature* 533, 333–337.
- Heiser, L.M., Sadanandam, A., Kuo, W.L., Benz, S.C., Goldstein, T.C., Ng, S., Gibb, W.J., Wang, N.J., Ziyad, S., Tong, F., et al. (2012). Subtype and pathway specific responses to anticancer compounds in breast cancer. *Proc. Natl. Acad. Sci. USA* 109, 2724–2729.
- Ioannidis, J.P. (2017). Acknowledging and overcoming nonreproducibility in basic and preclinical research. *JAMA* 317, 1019–1020.
- Kim, Y.M., Yang, S., Xu, W., Li, S., and Yang, X. (2008). Continuous in vitro exposure to low-dose genistein induces genomic instability in breast epithelial cells. *Cancer Genet. Cytogenet.* 186, 78–84.
- Lachmann, A., Giorgi, F.M., Alvarez, M.J., and Califano, A. (2016). Detection and removal of spatial bias in multiwell assays. *Bioinformatics* 32, 1959–1965.
- Lam, H.Y., Clark, M.J., Chen, R., Chen, R., Natsoulis, G., O'Huallachain, M., Dewey, F.E., Habegger, L., Ashley, E.A., Gerstein, M.B., et al. (2011). Performance comparison of whole-genome sequencing platforms. *Nat. Biotechnol.* 30, 78–82.
- List, M. (2017). Using docker compose for the simple deployment of an integrated drug target screening platform. *J. Integr. Bioinform.* 14.
- Marella, N.V., Malyavantham, K.S., Wang, J., Matsui, S., Liang, P., and Berezney, R. (2009). Cytogenetic and cDNA microarray expression analysis of MCF10 human breast cancer progression cell lines. *Cancer Res.* 69, 5946–5953.
- Mazoure, B., Nadon, R., and Makarenkov, V. (2017). Identification and correction of spatial bias are essential for obtaining quality data in high-throughput screening technologies. *Sci. Rep.* 7, 11921.
- Morrison, S.J. (2014). Time to do something about reproducibility. *eLife* 3.
- Muranen, T., Selfors, L.M., Worster, D.T., Iwanicki, M.P., Song, L., Morales, F.C., Gao, S., Mills, G.B., and Brugge, J.S. (2012). Inhibition of PI3K/mTOR leads to adaptive resistance in matrix-attached cancer cells. *Cancer Cell* 21, 227–239.
- Nature editorial. (2017). Replication studies offer much more than technical details. *Nature* 541, 259–260.
- Niepel, M., Hafner, M., Chung, M., and Sorger, P.K. (2017). Measuring cancer drug sensitivity and resistance in cultured cells. *Curr. Protoc. Chem. Biol.* 9, 55–74.
- Nosek, B.A., and Errington, T.M. (2017). Making sense of replications. *eLife* 6.
- Omberg, L., Ellrott, K., Yuan, Y., Kandoth, C., Wong, C., Kellen, M.R., Friend, S.H., Stuart, J., Liang, H., and Margolin, A.A. (2013). Enabling transparent and collaborative computational analysis of 12 tumor types within the Cancer Genome Atlas. *Nat. Genet.* 45, 1121–1126.
- Orth, J.D., Kohler, R.H., Fojer, F., Sorger, P.K., Weissleder, R., and Mitchison, T.J. (2011). Analysis of mitosis and antimitotic drug responses in tumors by *in vivo* microscopy and single-cell pharmacodynamics. *Cancer Res.* 71, 4608–4616.
- Peitz, O., Gilsdorf, M., and Boutros, M. (2010). Web cellHTS2: a web-application for the analysis of high-throughput screening data. *BMC Bioinformatics* 11, 185.
- Prinz, F., Schlange, T., and Asadullah, K. (2011). Believe it or not: how much can we rely on published data on potential drug targets? *Nat. Rev. Drug Discov.* 10, 712.
- Ramirez, M., Rajaram, S., Steininger, R.J., Osipchuk, D., Roth, M.A., Morinishi, L.S., Evans, L., Ji, W., Hsu, C.H., Thurley, K., et al. (2016). Diverse drug-resistance mechanisms can emerge from drug-tolerant cancer persisters cells. *Nat. Commun.* 7, 10690.
- Röyttä, M., Laine, K.M., and Häkkinen, P. (1987). Morphological studies on the effect of Taxol on cultured human prostatic cancer cells. *Prostate* 11, 95–106.
- Salani, B., Marini, C., Rio, A.D., Ravera, S., Massollo, M., Orengo, A.M., Amaro, A., Passalacqua, M., Maffioli, S., Pfeffer, U., et al. (2013). Metformin impairs glucose consumption and survival in Calu-1 cells by direct inhibition of hexokinase-II. *Sci. Rep.* 3, 2070.
- Sandve, G.K., Nekrutenko, A., Taylor, J., and Hovig, E. (2013). Ten simple rules for reproducible computational research. *PLoS Comput. Biol.* 9, e1003285.
- Schenone, M., Dančík, V., Wagner, B.K., and Clemons, P.A. (2013). Target identification and mechanism of action in chemical biology and drug discovery. *Nat. Chem. Biol.* 9, 232–240.
- Seashore-Ludlow, B., Rees, M.G., Cheah, J.H., Cokol, M., Price, E.V., Coletti, M.E., Jones, V., Bodycombe, N.E., Soule, C.K., Gould, J., et al. (2015). Harnessing connectivity in a large-scale small-molecule sensitivity dataset. *Cancer Discov.* 5, 1210–1223.
- Soliman, G.A., Steenson, S., and Etekpo, A. (2016). Effects of metformin and a mammalian target of rapamycin (mTOR) ATPCompetitive inhibitor on targeted metabolomics in pancreatic cancer cell line. *Mol Biol (Los Angel)*.

- Soule, H.D., Maloney, T.M., Wolman, S.R., Peterson, W.D., Jr., Brenz, R., McGrath, C.M., Russo, J., Pauley, R.J., Jones, R.F., and Brooks, S.C. (1990). Isolation and characterization of a spontaneously immortalized human breast epithelial cell line, MCF-10. *Cancer Res.* 50, 6075–6086.
- Tolliday, N. (2010). High-throughput assessment of Mammalian cell viability by determination of adenosine triphosphate levels. *Curr. Protoc. Chem. Biol.* 2, 153–161.
- Wilkinson, M.D., Dumontier, M., Aalbersberg, I.J., Appleton, G., Axton, M., Baak, A., Blomberg, N., Boiten, J.W., da Silva Santos, L.B., Bourne, P.E., et al. (2016). The FAIR Guiding Principles for scientific data management and stewardship. *Sci. Data* 3, 160018.
- Wilson, T.R., Fridlyand, J., Yan, Y., Penuel, E., Burton, L., Chan, E., Peng, J., Lin, E., Wang, Y., Sosman, J., et al. (2012). Widespread potential for growth-factor-driven resistance to anticancer kinase inhibitors. *Nature* 487, 505–509.
- Yonesaka, K., Zejnullahu, K., Lindeman, N., Homes, A.J., Jackman, D.M., Zhao, F., Rogers, A.M., Johnson, B.E., and Jänne, P.A. (2008). Autocrine production of amphiregulin predicts sensitivity to both gefitinib and cetuximab in EGFR wild-type cancers. *Clin. Cancer Res.* 14, 6963–6973.

STAR★METHODS**KEY RESOURCES TABLE**

REAGENT or RESOURCE	SOURCE	IDENTIFIER
Chemicals, Peptides, and Recombinant Proteins		
Horse Serum	Sigma-Aldrich	Cat # H1138, Lot # 12B496
Penicillin/Streptomycin	Invitrogen	Cat # 15070-063, Lot # 1697552
Hydrocortisone	Sigma-Aldrich	Cat # H-4001, Lot # SLBN5690V
Epidermal growth factor	R&D Systems	Cat # 236-EG, Lot # HLM7515071
Insulin	Sigma-Aldrich	Cat # I9278, Lot # SLBP1369V
Cholera toxin	Sigma-Aldrich	Cat # C8052, Lot # 095M4093V
Alpelisib	MedChem Express	Cat # HY-15244, Lot # 06192
Dasatinib	MedChem Express	Cat # HY-10191, Lot # 13044
Etoposide	MedChem Express	Cat # HY-13629, Lot # 11793
Neratinib	MedChem Express	Cat # HY-32721, Lot # 10283
Paclitaxel	MedChem Express	Cat # HY-B0015, Lot # 18138
Palbociclib	MedChem Express	Cat # HY-50767, Lot # 16349
Trametinib	MedChem Express	Cat # HY-10999, Lot # 07378
Vorinostat	MedChem Express	Cat # HY-10221, Lot # 09386
Deposited Data		
Mean GR values and metrics for all Centers	this paper	Synapse: syn18478968
GR values and metrics for all Centers/Scientists	this paper	Synapse: syn18475380
GR values and metrics for timecourse	this paper	Synapse: syn18478971
Experimental Models: Cell Lines		
MCF10A	ATCC	CRL-10317; RRID CVCL_0598
MCF 10A-H2B-mCherry	Hafner et al. 2016	N/A
Software and Algorithms		
MATLAB (R2016b)	MathWorks	https://mathworks.com/products/matlab.html
Columbus (v2.7.0)	Perkin Elmer, Waltham, MA	http://perkinelmer.com/product/image-data-storage-and-analysis-system-columbus
DataRail	Hafner et al. 2017b	https://github.com/datarail/datarail

LEAD CONTACT AND MATERIALS AVAILABILITY

Further information and requests for resources and reagents should be directed to, and will be fulfilled by, the Lead Contact, Laura Heiser (heiserl@ohsu.edu).

Materials Availability Statement

This study did not generate new unique reagents.

EXPERIMENTAL MODEL AND SUBJECT DETAILS

Three isolates of the non-malignant female human breast epithelial MCF 10A cell line, here referred to as MCF 10A-GM, MCF 10A-OHSU, and MCF 10A-HMS, were sourced independently from the ATCC and then passaged in separate institutions; use of these lines was intended to replicate the common practice of maintaining local cell stocks. MCF 10A-H2B-mCherry cells were created by inserting an H2B-mCherry expression cassette into the AAVS1 safe harbor genomic locus of MCF 10A-HMS using CRISPR/Cas9 ([Hafner et al., 2016](#)). All lines were confirmed to be MCF 10A cells by STR profiling ([Table S1](#)), and confirmed to have stable karyotypes by g-banding 47,XX,i(1)(q10),+del(1)(q12q32),add(3)(p13),add(8)(p23),add(9)p(14). All lines were cultured in DMEM/F12 base media (Invitrogen #11330-032) supplemented with 5% horse serum, 0.5 µg/mL hydrocortisone, 20 ng/mL rhEGF, 10 µg/mL

insulin, 100 ng/mL cholera toxin, and 100 units/mL penicillin and 100 µg/mL streptomycin as described previously (Debnath et al., 2003). Base media, horse serum, hydrocortisone, rhEGF, insulin, and cholera toxin were purchased by the MEP-LINCS Center and distributed to the remaining experimental sites. MCF 10A-GM was expanded by Gordon Mills at MD Anderson Cancer Center and distributed to all experimental sites. Cell identity was confirmed at individual experimental sites by short tandem repeat (STR) profiling, and the cells were found to be free of mycoplasma prior to performing experiments.

METHOD DETAILS

The experimental and computational protocols to measure drug response are described in detail in two prior publications (Hafner et al., 2017b; Niepel et al., 2017). The following protocol (available in full below) was suggested for this study: cells were plated at 750 cells per well in 60 µL of media in 384-well plates using automated plate fillers and incubated for 24 h prior to drug addition. Drugs were added at the indicated doses with a D300 Digital Dispenser (Hewlett-Packard), and cells were further incubated for 72 h. At the time of drug addition and at the endpoint of the experiment, cells were stained with Hoechst and LIVE/DEAD™ Fixable Red Dead Cell Stain (Thermo Fisher Scientific) and cell numbers were determined by imaging as described (Hafner et al., 2016; Niepel et al., 2017) or by the CellTiter-Glo assay (Promega). Some details of the experimental protocol differed across Centers and over time, e.g., manually dispensing of drugs or use of 96-well plates. The data included in Figures 1C and S2 (Scientist C) were collected for a separate project using different stocks of consumable reagents, and included here as an additional comparison. In these experiments, cells were treated via pin transfer, and HMS isolate 3 MCF10A cells were used.

For live-cell experiments with MCF 10A-H2B-mCherry, cell counts were performed by imaging plates in an 2 hr interval over the course of 96 hours (only first 50 hours shown) (Hafner et al., 2016; Niepel et al., 2017). Data analysis was performed as described previously (Hafner et al., 2016; Niepel et al., 2017).

The evaluation of irregularities in growth across microtiter plates was performed by plating MCF 10A cells at 750 cells per well in 60 µL of media in 384-well plates using automated plate fillers and determining cell numbers after 96 h through imaging as described (Hafner et al., 2016; Niepel et al., 2017).

Drugs were obtained from commercial vendors by HMS LINCS, tested for identity and purity by LC/MS in house as described in detail in the drug collection section of the HMS LINCS Database (<http://lincs.hms.harvard.edu/db/sm/>), and distributed as 10 mM stock solutions dissolved in DMSO to all experimental sites. See **Key Resources Table** for additional metadata.

Measuring Drug Responses – SOP

General Considerations

The two main considerations in measuring drug responses in cell lines are that the results are reproducible and representative of the relevant underlying biology of the system. To improve reproducibility we point out specific experimental steps that are prone to introducing variability and articulate what steps can be taken to minimize this variability. To ensure that the results are representative of the underlying biology we point out specific experimental conditions that should be optimized for each drug-cell line condition. For example, some drug-cell line interactions change with cell density and/or are dependent on cell state, so it is important to maintain constant plating numbers within an appropriate density range from one experiment to the next. Although always plating cells at high density so there is little or no growth might produce reproducible results that suggest a cell line is resistant to drug, this result would not necessarily be representative of how the drug actually acts on dividing cells. Experimental design therefore must achieve both goals - reproducibility and representativeness.

Automation is one key way to improve reproducibility. In particular when working with 384 well plates any form of manual manipulation will introduce unacceptable levels of variation. Ideally, every step (plating, treatment, measurement, and analysis) should be automated to reduce user-induced artifacts.

Step-By-Step Protocol

Plating Cells.

- 1) Grow MCF10A cells following protocol provided by Gray/Mills.
 - a) It is important the cells are in mid-log phase and not in a state of arrest or quiescence since they will otherwise need more than 24 hours to become proliferative again.
- 2) Harvest and count cells following protocol provided by Gray/Mills.
 - a) Make sure that during the detaching process all cells get harvested and that the cells do not clump which will make accurate counting and dispensing difficult.
 - b) Cells should quickly be brought up in complete growth media and traces of detaching solution should be removed by centrifugation to minimize stress for the cells.
 - c) Automated cell counters may not give the most accurate counts, but they will speed up the process when many cell solutions need to be counted and they will improve reproducibility
- 3) Plate cells at 750 cells/well in 60-ul complete media in four standard 384 well plates compatible with downstream assay of cell number. (ALTERNATIVE – Plate 2250 cells/well in 200ul media if using 96 well plates.)
 - a) An accurate count here is not sufficient to estimate the number of cells in the well at the time of drug treatment. There is too much variability in the the number of cells that actually adhere and the time it takes for cells to start growing after plating. We therefore use one plate of the four plates to obtain an accurate pre-treatment cell count.

- a) Especially for sensitive cells it is important to stain for dead cells to ensure that the correct number of live cells gets plated.
 - b) Ideally use a fully automated cell dispenser.
 - c) Take care to gently resuspend cells if plating takes more than a couple of minutes as cells will settle which will lead to uneven dispensing.
 - d) Place plates on a benchtop, sheltered from direct warm or cool air from the heating system, for 20 minutes to allow the cells to settle. Cells may distribute unevenly if they are placed directly in the incubator due to vibration of the shelves.
 - e) Move plates to an incubator. If the incubator is opened often, it is advisable to place plates into secondary containment (we use a tupperware container lined with moist paper towels) to reduce temperature and CO₂ fluctuations, in particular of the edge wells.
- 4) Incubate cells for 24 hours.
- a) Cells will show a bit of a lag phase after plating, either due to a slowdown of growth during the expansion of the cells or due to stress induced by plating. It is advisable to observe for a new cell line if cells are actively cycling after plating.
 - b) We have observed some synchronization after cell plating as well. Again, this is likely due to a cell cycle arrest present in the cells at the time of plating.

Treating Cells.

- 5) Treat cells in three plates with drugs in a nine-point SQRT(10)-fold dilution series covering four orders of magnitude starting at the highest dose according to the table below using an HP D300 Drug Dispenser.
 - a) The time of addition of drug is considered t=0.
 - b) The experimental design should be such that the three plates represent a technical triplicate of the overall experiment. Since there is plate-to-plate variation it is best to have the technical repeats on different plates.
 - c) Automation is the most important feature. And ideally, we want to minimize the addition of extraneous media. So treatment with a D300 or pin transfer is ideal.
 - d) If no D300 drug dispenser is available, prepare the drugs at the right concentration and transfer them in 10 µl into each well using a multi-channel pipette.
- 6) At time t=0 assay the fourth (untreated control) plate (see below).
- 7) Incubate the treated cells for up to an additional 72 hours.
 - a) Ensure that in the DMSO-treated control wells cells are still dividing actively at the end of the experiment.
 - b) Fast growing cell lines can be measured after two days while slower growing lines can be incubated for three or even four days.
- 8) At time t=3 days assay the technical triplicate plates (see below).

Measuring Cell Numbers.

- 9) At the indicated time points perform your preferred assay to determine the relative cell number for each well.
 - a) The preferred method to analyze cell number is to count them by microscopy assays to get a direct count of viable cells (see assay below).
 - b) ALTERNATIVE – Proxy assays such as CellTiter-Glo or AlamarBlue will work for the GR calculations, however DNA, ATP, or other proxy-markers may be affected by drug response independent of the actual cell number.
- 10) Add 20µl of staining solution (1:1000 LIVE/DEAD Far Red Dead Cell Stain (Thermo Fisher Scientific, L-34974), 2 µM Hoechst 33342 (Thermo Fisher Scientific, 62249), 10% OptiPrep (Sigma-Aldrich, D1556-250ML) in PBS). Incubate for 30min at RT. Add 20µl of fixing solution (3% formaldehyde (Sigma Aldrich, F8775-500ML), 20% OptiPrep (Sigma-Aldrich, D1556-250ML) in PBS). Incubate for 30min at RT. Remove 90µl of supernatant and replace with 90µl of PBS and proceed to scanning.
 - a) NOTE – Add the staining and fixing solution with an automated pipettor, holding it at an approximately 45 degree angle and touching the side wall of the tube. The solutions should run down the side wall of the well and accumulate at the bottom of the well due to their increasing density.
 - b) ALTERNATIVE – Stain and fix cells by adding 20µl of 8 µM Hoechst 33342 (Thermo Fisher Scientific, 62249) in 12% formaldehyde (Sigma Aldrich, F8775-500ML). Incubate for at least 1h before proceeding to scan. This method does not distinguish between live and dead cells directly, even though apoptotic cells should have grossly altered morphology which can be recognized by image analysis software.
- 11) Scan each treated well of the 384 well plates.
 - a) If possible, scan the entire well area to improve count accuracy for low cell numbers or unevenly distributed cells.
- 12) Use your favorite image analysis algorithms to count live cells.
 - a) Use a standard nuclei detection algorithm. Be sure to impose min/max levels for area or brightness to exclude nuclear fragments.
 - b) If using the LIVE/DEAD stain, do not count any nuclei that are LIVE/DEAD-positive.

Record Results.

- 13) Record the measured cell numbers or proxy measurements according to the DR2.0 standards.
- Data standards are detailed in a separate document.
 - Be sure to record all necessary pieces of information so the results from different Centers can be aggregated and compared

Calculating Drug Sensitivity.

- 14) Calculate growth-rate inhibition (GR) values for each drug dose and fit the resulting curve with a sigmoid to extract GR₅₀, GR_{inf}, and GR_{hill}.
- Calculation of GR metrics are detailed in a separate document.

Drug Information.

Drug	HMSLid	Primary target	Highest dose (uM)	Stock (mM)
Paclitaxel	10102	microtubules	1	10
Alpelisib/BYL719	10233	PI3Ka	10	10
Neratinib/HKI272	10018	EGFR/HER2	3.16	10
Dasatinib	10020	BCR/ABL	10	10
Trametinib/GSK1120212	10142	MEK	1	10
Palbociclib/PD0332991	10071	CDK4/6	3.16	10
Vorinostat	10282	HDAC	10	10
Etoposide	10250	Topoisomerase	10	10

QUANTIFICATION AND STATISTICAL ANALYSIS

The technical variability associated with data collected by each Center or scientist in Center one was computed for each drug-dose pair as the standard error (SE; [Equation 1](#)) in GR value across all technical replicates per biological replicate. Note that GR values, not GR metrics derived from curve fitting were used for this calculation. The number of data points considered for calculating SE in technical replicates varied by Center/scientist and is shown in the table under the column “# Technical replicates per biological replicate”. The number of SE values per drug-dose pair is equal to the number of biological replicates. For example, the distribution of standard error (technical replicates) for Center 1, Scientist B is made up of 192 SE data points (8 drugs * 8 doses * 3 biological replicates).

$$SE = \frac{\sigma}{\sqrt{n}} \quad \text{Equation 1a}$$

$$\sigma = \sqrt{\frac{\sum (x_i - \mu)^2}{n - 1}} \quad \text{Equation 1b}$$

For a given drug-dose pair, σ is the standard deviation computed across GR values, n is the number of technical or biological replicates, x_i is the GR value measured in a certain replicate i , μ is the mean GR value across replicates.

The biological variability of each Center or scientist was also computed for each drug-dose pair as the standard error (SE; [Equation 1](#)) in GR value across all biological replicates such that each SE computation was based on data from only one technical replicate per biological replicate. The number of data points used to compute each SE value is equal to the number of biological replicates. The

number of SE values per drug-dose pair is equal to $\binom{t}{1}^b$ or t^b where b is the number of biological replicate plates, t is the number of technical replicates per biological replicate. For example, the number of SE values (data points) computed per drug-dose pair for Center 1, Scientist B is $3^3 = 27$. The total number of drug-dose pairs in a complete dataset for each Center is 64. Hence, the distribution of standard error for biological replicates associated with data collected in Center 1 by Scientist B is computed from 1728 data points.

Center/Scientist	# Technical replicates per biological replicate	# Biological replicates
Center 1, Scientist A (2019)	9 (3 wells x 3 plates)	3
Center 1, Scientist A (2017)	2	3
Center 1, Scientist B	9 (3 wells x 3 plates)	3
Center 1, Scientist C	4	2
Center 2	4	1
Center 3	3	2
Center 4	3	2
Center 5	2	2

DATA AND CODE AVAILABILITY

Analysis of variability in GR values or metrics measured across centers is recorded in Jupyter notebooks. These notebooks document blocks of executable code alongside human-readable descriptions of the methods used to compute variability, and can be re-run by the reader to reproduce the results described. Jupyter notebooks for experimental design and data analysis are available: https://github.com/labsyspharm/MCF10A_DR_reproducibility and <https://github.com/datarail/datrail>.

The data from each Center and a list of best practices are available at <http://www.grcalculator.org/grbrowser/> under ‘LINCS MCF10A Common Project’.

The data from Scientist C are available: <http://lincs.hms.harvard.edu/db/datasets/20343/> and <http://lincs.hms.harvard.edu/db/datasets/20344/>

All data have also been deposited on Synapse: (synapse.org) syn18456348. The final drug response results (mean GR values and GR metrics) generated by all LINCS Centers (Related to [Figure 5](#)) are under Synapse: syn18478968. The time course data (Related to [Figures 4 and S5](#)) are under Synapse: syn18478971. All technical and biological GR values for each Center (Related to [Figures 5 and S6](#)) are under Synapse: syn18475380.

Supplemental Information

**A Multi-center Study on the Reproducibility
of Drug-Response Assays in Mammalian Cell Lines**

Mario Niepel, Marc Hafner, Caitlin E. Mills, Kartik Subramanian, Elizabeth H. Williams, Mirra Chung, Benjamin Gaudio, Anne Marie Barrette, Alan D. Stern, Bin Hu, James E. Korkola, LINCS Consortium, Joe W. Gray, Marc R. Birtwistle, Laura M. Heiser, and Peter K. Sorger

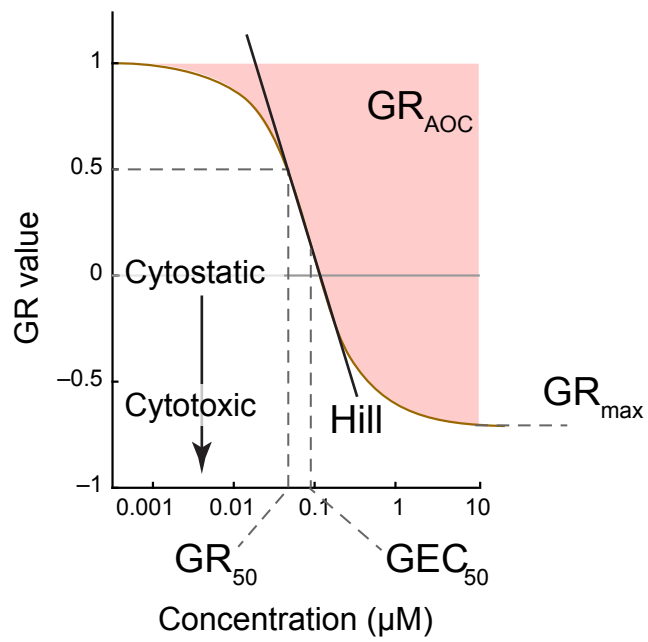


Figure S1, Related to Figure 1

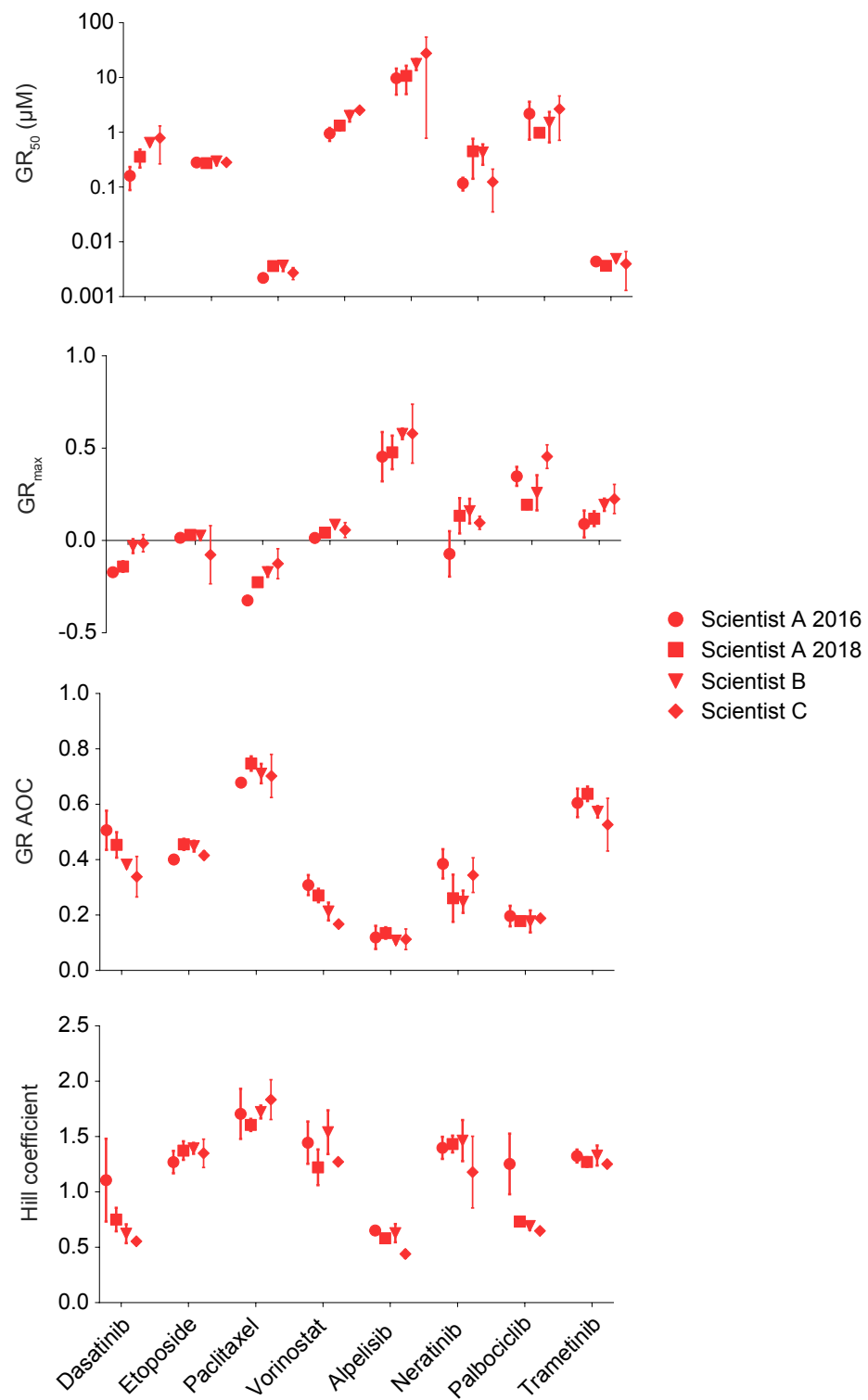
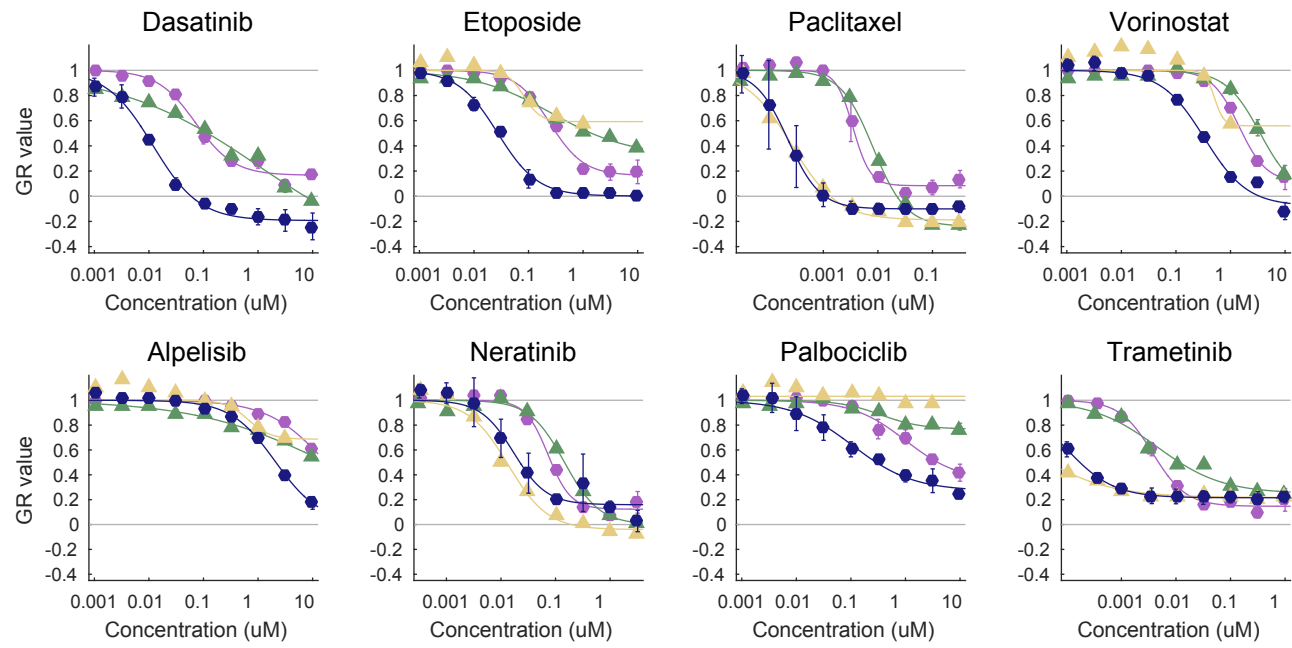


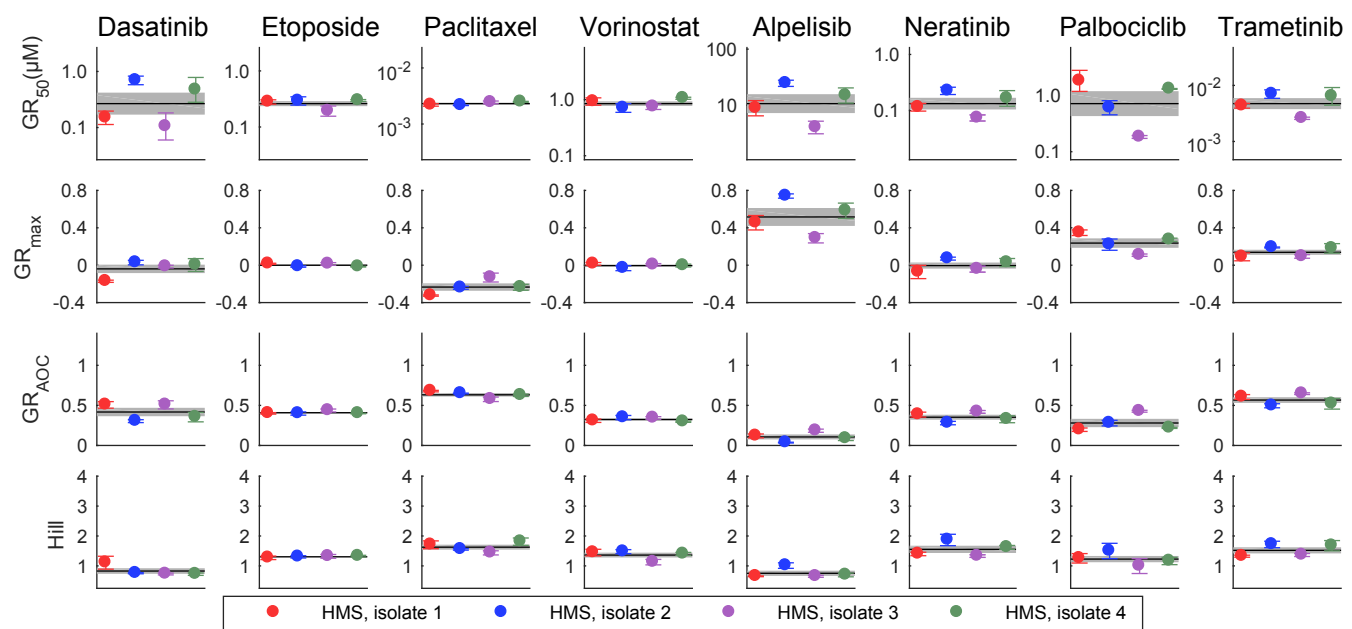
Figure S2, Related to Figure 2



	Drug dilution performed at:	Cell culture performed at:	Readout assay:	
Preliminary 1	Center 3	Center 3	Imaging	—●—
Preliminary 2	Center 3	Center 4	CTG	—▲—
Center 3	Center 3	Center 3	Imaging	—○—
Center 4	Center 4	Center 4	CTG	—△—

Figure S3, Related to Figure 3

A



B

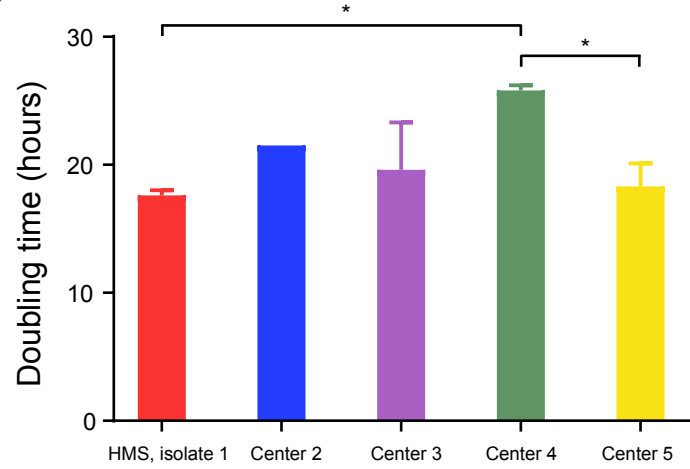


Figure S4, Related to Figure 3

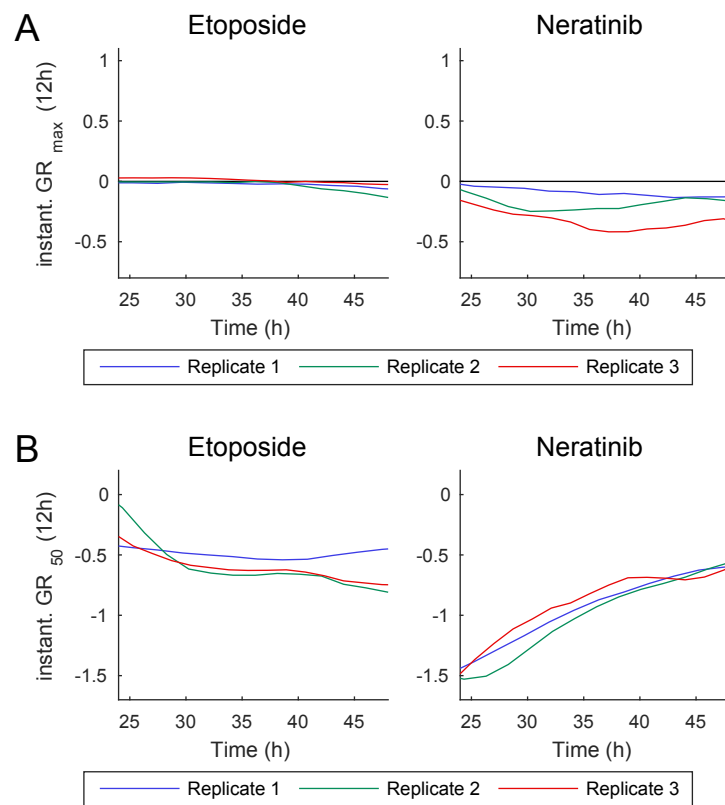


Figure S5, Related to Figure 4

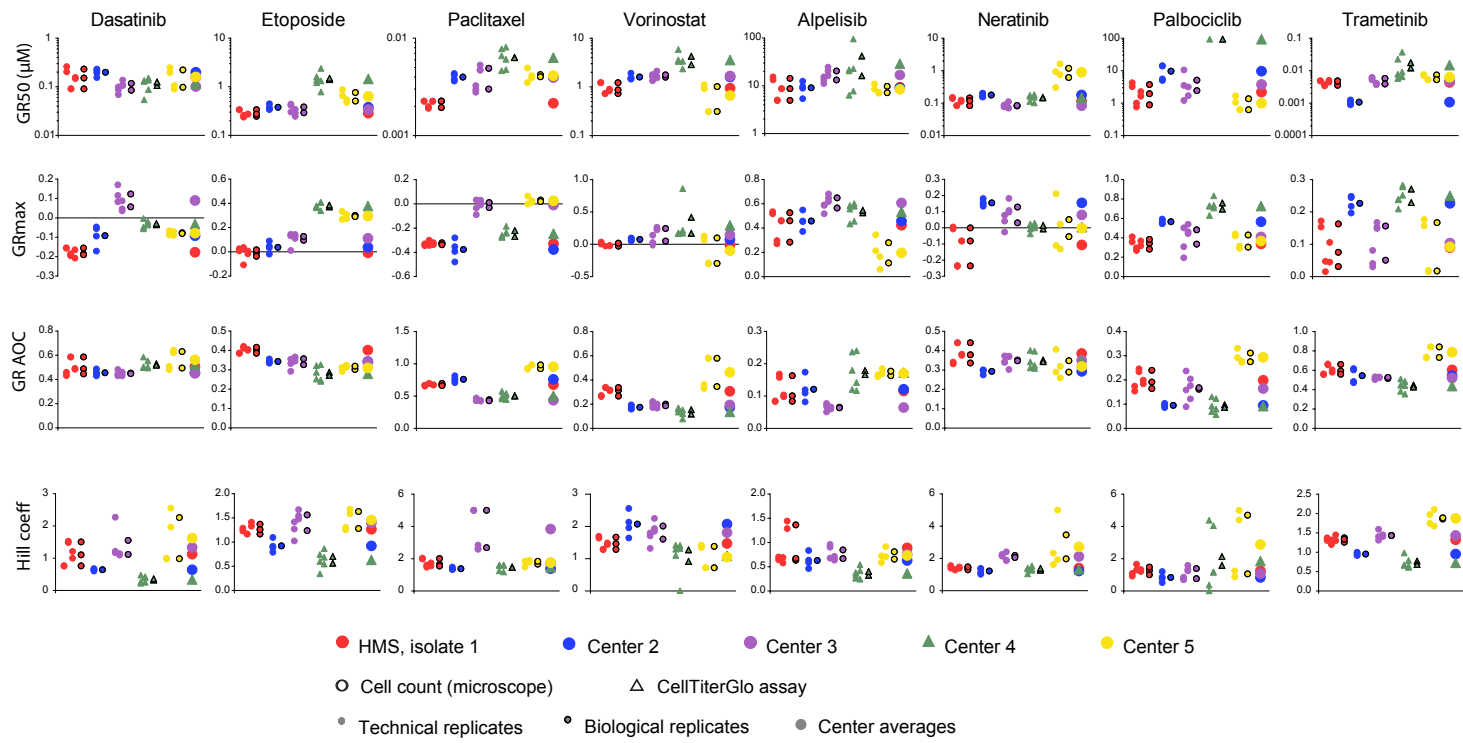


Figure S6, Related to Figure 6

Supplemental Figure Legends

Figure S1, Related to Figure 1: GR dose-response curve and metrics

Schematic of a dose-response curve under the GR model and the source of the derived metrics.

Figure S2, Related to Figure 2: Assay stability over time

GR metrics of MCF 10A cells treated with each drug showing the mean and standard deviation of biological triplicates collected by an experienced research scientist (Scientist A, circles), by the same scientist two years later (squares), by a new technician two years later (Scientist B, triangles), and biological duplicates collected as part of a separate LINCS project in Center One (<http://lincs.hms.harvard.edu/db/datasets/20344/>) (Scientist C).

Figure S3, Related to Figure 3: GR metrics describing the initial experiments to assess sensitivity of MCF 10A cells to eight drugs measured at three Centers. Center Three and Center Four represent the final results provided by each Center and are the same data presented in Figure 6A. Preliminary 1 represents initial experiments run by Center Three, which showed poor agreement with data from the other two Centers (see table for pipeline details). The disparate results reflect in part differences in readout (CTG vs. Imaging) for Etoposide, Vorinostat, Alpelisib, and Palbociclib. Preliminary 2 represents a coordinated effort by Centers Three and Four: daughter drug plates used by Center Three in Preliminary 1 experiments were shipped to Center Four for cell culture. For many drugs, there is good agreement between Preliminary 1 and Preliminary 2, indicating consistency between cell culturing. The consistent discrepancy in responses to Trametinib between Preliminary 1-Preliminary 2 studies and Center Three-Center Four studies indicate errors in construction of the drug dilution series.

Figure S4, Related to Figure 3: GR metrics across MCF 10A isolates

(A) GR metrics describing the sensitivity of four different MCF 10A cell isolates to eight drugs measured independently at the HMS LINCS center. The black line shows the mean sensitivity measured across all isolates, and the gray box shows the standard error of the mean. (B) The doubling time of MCF10A cells at each LINCS Center. The error bars represent the standard deviation of the mean, the * indicates P<0.05 by one way ANOVA with Tukey's multiple comparison tests.

Figure S5, Related to Figure 4: Instantaneous GR metrics

Instantaneous GR_{max} (A) and GR₅₀ (B) values in MCF 10A cells treated with Etoposide (left) and Neratinib (right) over the course of 24 hrs for three biological repeats.

Figure S6, Related to Figure 6: Technical and biological variability in GR metrics across Centers

GR metrics for all technical and biological replicates of MCF 10A cells treated with eight drugs by five LINCS Centers (circles represent data from image-based assays and triangles from CellTiter-Glo® assays).

Supplemental Tables

Table S1, Related to STAR Methods: STR profiling results for all MCF 10A isolates used.

Sample Name	Comment	Marker	Allele	Allele	Peak Height	Peak Height
			1	2	Allele 1	Allele 2
NTC	no template control	TH01	0	0		
NTC	no template control	D21S11	0	0		
NTC	no template control	D5S818	0	0		
NTC	no template control	D13S317	0	0		
NTC	no template control	D7S820	0	0		
NTC	no template control	D16S539	0	0		
NTC	no template control	CSF1PO	0	0		
NTC	no template control	Amelogenin				
NTC	no template control	vWA	0	0		
NTC	no template control	TPOX	0	0		
2800M_pos_ctrl	positive control	TH01	6	9.3	2105	2151
2800M_pos_ctrl	positive control	D21S11	29	31.2	1716	1751
2800M_pos_ctrl	positive control	D5S818	12		6411	
2800M_pos_ctrl	positive control	D13S317	9	11	1919	1757
2800M_pos_ctrl	positive control	D7S820	8	11	2650	2704
2800M_pos_ctrl	positive control	D16S539	9	13	2911	2766
2800M_pos_ctrl	positive control	CSF1PO	12		6539	
2800M_pos_ctrl	positive control	Amelogenin	X	Y	1692	1659
2800M_pos_ctrl	positive control	vWA	16	19	724	696
2800M_pos_ctrl	positive control	TPOX	11		2550	
MCF10A-HMS_1	replicate 1	TH01	8	9.3	309	238
MCF10A-HMS_1	replicate 1	D21S11	28	30	295	259
MCF10A-HMS_1	replicate 1	D5S818	10	13	529	1018
MCF10A-HMS_1	replicate 1	D13S317	8	9	280	349
MCF10A-HMS_1	replicate 1	D7S820	10	11	609	525
MCF10A-HMS_1	replicate 1	D16S539	11	12	358	379
MCF10A-HMS_1	replicate 1	CSF1PO	10	12	496	945
MCF10A-HMS_1	replicate 1	Amelogenin	X		488	
MCF10A-HMS_1	replicate 1	vWA	15	17	132	118
MCF10A-HMS_1	replicate 1	TPOX	9	11	191	155
MCF10A-HMS_2	replicate 2	TH01	8	9.3	294	317
MCF10A-HMS_2	replicate 2	D21S11	28	30	327	298
MCF10A-HMS_2	replicate 2	D5S818	10	13	550	1046
MCF10A-HMS_2	replicate 2	D13S317	8	9	347	314
MCF10A-HMS_2	replicate 2	D7S820	10	11	665	429
MCF10A-HMS_2	replicate 2	D16S539	11	12	532	560
MCF10A-HMS_2	replicate 2	CSF1PO	10	12	568	1096
MCF10A-HMS_2	replicate 2	Amelogenin	X		489	
MCF10A-HMS_2	replicate 2	vWA	15	17	173	112
MCF10A-HMS_2	replicate 2	TPOX	9	11	152	192
MCF10A-H2B-mCherry_1	replicate 1	TH01	8	9.3	288	229
MCF10A-H2B-mCherry_1	replicate 1	D21S11	28	30	272	276
MCF10A-H2B-mCherry_1	replicate 1	D5S818	10	13	363	904
MCF10A-H2B-mCherry_1	replicate 1	D13S317	8	9	205	273

Sample Name	Comment	Marker	Allele	Allele	Peak Height	Peak Height
			1	2	Allele 1	Allele 2
MCF10A-H2B-mCherry_1	replicate 1	D7S820	10	11	341	420
MCF10A-H2B-mCherry_1	replicate 1	D16S539	11	12	400	371
MCF10A-H2B-mCherry_1	replicate 1	CSF1PO	10	12	520	807
MCF10A-H2B-mCherry_1	replicate 1	Amelogenin	X		353	
MCF10A-H2B-mCherry_1	replicate 1	vWA	15	17	104	97
MCF10A-H2B-mCherry_1	replicate 1	TPOX	9	11	140	122
MCF10A-H2B-mCherry_2	replicate 2	TH01	8	9.3	178	183
MCF10A-H2B-mCherry_2	replicate 2	D21S11	28	30	200	197
MCF10A-H2B-mCherry_2	replicate 2	D5S818	10	13	256	495
MCF10A-H2B-mCherry_2	replicate 2	D13S317	8	9	158	227
MCF10A-H2B-mCherry_2	replicate 2	D7S820	10	11	380	374
MCF10A-H2B-mCherry_2	replicate 2	D16S539	11	12	262	265
MCF10A-H2B-mCherry_2	replicate 2	CSF1PO	10	12	283	664
MCF10A-H2B-mCherry_2	replicate 2	Amelogenin	X		230	
MCF10A-H2B-mCherry_2	replicate 2	vWA	15	17	79	76
MCF10A-H2B-mCherry_2	replicate 2	TPOX	9	11	125	94
MCF10A-OHSU_1	replicate 1	TH01	8	9.3	195	236
MCF10A-OHSU_1	replicate 1	D21S11	28	30	236	217
MCF10A-OHSU_1	replicate 1	D5S818	10	13	362	766
MCF10A-OHSU_1	replicate 1	D13S317	8	9	220	257
MCF10A-OHSU_1	replicate 1	D7S820	10	11	430	433
MCF10A-OHSU_1	replicate 1	D16S539	11	12	399	262
MCF10A-OHSU_1	replicate 1	CSF1PO	10	12	428	840
MCF10A-OHSU_1	replicate 1	Amelogenin	X		397	
MCF10A-OHSU_1	replicate 1	vWA	15	17	88	111
MCF10A-OHSU_1	replicate 1	TPOX	9	11	130	125
MCF10A-OHSU_2	replicate 2	TH01	8	9.3	267	261
MCF10A-OHSU_2	replicate 2	D21S11	28	30	291	313
MCF10A-OHSU_2	replicate 2	D5S818	10	13	500	1000
MCF10A-OHSU_2	replicate 2	D13S317	8	9	262	328
MCF10A-OHSU_2	replicate 2	D7S820	10	11	622	407
MCF10A-OHSU_2	replicate 2	D16S539	11	12	396	368
MCF10A-OHSU_2	replicate 2	CSF1PO	10	12	431	789
MCF10A-OHSU_2	replicate 2	Amelogenin	X		485	
MCF10A-OHSU_2	replicate 2	vWA	15	17	157	150
MCF10A-OHSU_2	replicate 2	TPOX	9	11	231	201
MCF10A-GM_1	replicate 1	TH01	8	9.3	256	196
MCF10A-GM_1	replicate 1	D21S11	28	30	297	252
MCF10A-GM_1	replicate 1	D5S818	10	13	628	1394
MCF10A-GM_1	replicate 1	D13S317	8	9	431	366
MCF10A-GM_1	replicate 1	D7S820	10	11	679	463
MCF10A-GM_1	replicate 1	D16S539	11	12	519	497
MCF10A-GM_1	replicate 1	CSF1PO	10	12	654	1266
MCF10A-GM_1	replicate 1	Amelogenin	X		729	
MCF10A-GM_1	replicate 1	vWA	15	17	149	159
MCF10A-GM_1	replicate 1	TPOX	9	11	174	177

Sample Name	Comment	Marker	Allele	Allele	Peak Height	Peak Height
			1	2	Allele 1	Allele 2
MCF10A-GM_2	replicate 2	TH01	8	9.3	452	389
MCF10A-GM_2	replicate 2	D21S11	28	30	505	576
MCF10A-GM_2	replicate 2	D5S818	10	13	943	1395
MCF10A-GM_2	replicate 2	D13S317	8	9	489	461
MCF10A-GM_2	replicate 2	D7S820	10	11	890	755
MCF10A-GM_2	replicate 2	D16S539	11	12	713	591
MCF10A-GM_2	replicate 2	CSF1PO	10	12	676	1415
MCF10A-GM_2	replicate 2	Amelogenin	X		893	
MCF10A-GM_2	replicate 2	vWA	15	17	268	210
MCF10A-GM_2	replicate 2	TPOX	9	11	240	278